

1 **Title:** Benthic food resources and the condition of benthic-demersal fish: spatial trends and relationships
2 in the northern shelf of the Bay of Biscay.

3

4 **Authors:** Thomas Outrequin¹, Hubert du Pontavice ², Jérôme Guitton¹, Pauline Boët¹, Jacques Grall³,
5 Pascal Laffargue¹, Hervé Le Bris¹

6

7 **Affiliation:**

8 1. DECOD (Ecosystem Dynamics and Sustainability), Institut Agro, IFREMER, Rennes, Nantes, France

9 2. IFREMER, HMMN, Laboratoire Ressources Halieutiques, F-14520 Port en Bessin, France

10 3. OSU UAR 313 IUEM, Univ Brest, CNRS, IRD, 29280 Plouzané, France

11 The authors made the following contributions. Thomas Outrequin: Conceptualization, Writing - Original
12 Draft, Writing - Review and Editing; Hubert Du Pontavice: Conceptualization and Investigation; Jérôme
13 Guitton: Methodology and Resources; Pauline Boët: Investigation and Resources; Jacques Grall:
14 Writing - Review and Editing, Supervision; Pascal Laffargue: Writing - Review and Editing, Supervision;
15 Hervé Le Bris: Writing - Review and Editing, Supervision.

16 Correspondence concerning this article should be addressed to Thomas Outrequin.

17 Postal address: 65 rue de Saint-Brieuc, Rennes, 35000, France

18 E-mail: thomas.outrequin@institut-agro.fr

19 **Abstract:**

20 To understand the trophic functioning of continental shelves, it is necessary to evaluate the factors that
21 drive production at different levels. For benthic-demersal fish, one such factor is spatial variability in the
22 biomass of their macrobenthic prey. In this study, we investigated the distribution of the macrobenthos
23 in the northern part of the continental shelf of the Bay of Biscay in order to determine how variability in
24 these prey resources might affect the benthic-demersal fish that feed on them. Due to the scarcity of
25 available field data, an empirical graph model and a biochemical model were used to produce different
26 indices of macrobenthic biomass, which were then used to generate three maps illustrating the
27 distribution of this biomass in the Bay of Biscay. In general, values from these maps showed high
28 Spearman correlations with the limited data available, but also discrepancies at greater depths where
29 field data are quite poor. Globally, a pronounced decline in macrobenthic biomass was observed from
30 the coast to offshore, but with particularly high values in deeper muddy sediments. Among eight fish
31 species analyzed, the four most known for their strongly benthivorous diet demonstrated positive
32 relationships between body condition and the macrobenthic biomass indices, with the strongest
33 associations detected for smaller-sized fish. This suggests that biomass index maps may be i) indicative
34 of the availability of benthic prey at the level of the continental shelf along a major coastal-offshore
35 gradient, and ii) useful for studying spatial variability in the transfer of energy or matter along the food
36 chain within this ecosystem. However, there is a clear need for macrobenthic data from field surveys at
37 the shelf scale, notably in deep circalittoral areas, to confirm or improve the accuracy of the spatial
38 biomass trends estimated by models.

39 **Highlights:**

- 40 - Estimates of macrobenthic biomass exhibited coastal-to-offshore trend on the shelf.
- 41 - The sparse field data macrobenthic biomass correlated with data from models.
- 42 - In deeper areas, muddy sediments contained the greatest macrobenthic biomass.
- 43 - Body condition of benthivorous fish improved with increased macrobenthic biomass.
- 44 - Diet literature suggests biomass maps reflect food resources beyond macrofauna.

45 **Key words:** Macrobenthic biomass, fish, body condition, continental shelf, food resource, Bay of
46 Biscay

47

48 **Introduction**

49 The northwest Atlantic shelf is a vast area whose location between the continent and the ocean creates
50 strong environmental gradients that influence ecological processes such as matter production and
51 transfer (Hall, 2002). Within this ecosystem, benthic invertebrates play a preeminent role as a link
52 between primary producers and top predators (Chen et al., 2021), particularly benthic-demersal fish.
53 From the coast to the shelf break, strong declining gradients are typically observed in levels of nutrients,
54 organic matter, and primary production, and it is generally assumed that the biomass and/or production
55 of benthic invertebrates follow the same trend (Hall, 2002; Wei et al., 2010). Given the role of these
56 invertebrates as prey for benthic-demersal fish (Amezcuca et al., 2003; Armstrong, 1982; Day et al.,
57 2019), it is likely that such spatial trends in food resources will have repercussions for fish populations
58 across the continental shelf.

59 The northern part of the continental shelf of the Bay of Biscay offers an ideal location to study spatial
60 trends in these prey resources--particularly in the macrobenthic component--and the consequences for
61 the benthic-demersal fish that depend on them for food (e.g., Lagardère, 1987; Le Loc'h and Hily, 2005).
62 In this area, there is a strong terrigenous influence from the numerous small coastal rivers that flow onto
63 the coastal fringe as well as two larger rivers, the Vilaine and the Loire (Borja et al., 2019). Given this, it
64 is logical to expect a coastal-to-offshore gradient in the production or biomass of benthic invertebrates.
65 However, to confirm this kind of trend, it would be necessary to have data covering the entire study area,
66 as was done in the North Sea by Reiss et al. (2010). Unfortunately, the available data on macrobenthic
67 biomass in the Bay of Biscay are scattered in time and mainly restricted to coastal areas or to specific
68 shelf habitats (e.g., mid-shelf fishing grounds) (Kopp et al., 2015; Le Loc'h et al., 2008; Rigolet et al.,
69 2014; Robert, 2017). In such a case, though, it may be possible to estimate biomass using established
70 models, such as the empirical model developed by Chassé and Glémarec (1976) based on depth and
71 sedimentary substrates. More recently, mechanistic models like ERSEM (Kay et al., 2018) have also
72 shown promise for predicting the spatial variability of macrobenthic biomass (e.g., Timmermann et al.,
73 2012).

74 Higher-quality habitats, such as those offering more food resources, are generally associated with
75 improved body condition among predators (Engelhard et al., 2013; Liao et al., 1995). Therefore, it may
76 be that patterns of abundance or scarcity of macrofaunal food resources across the shelf could translate

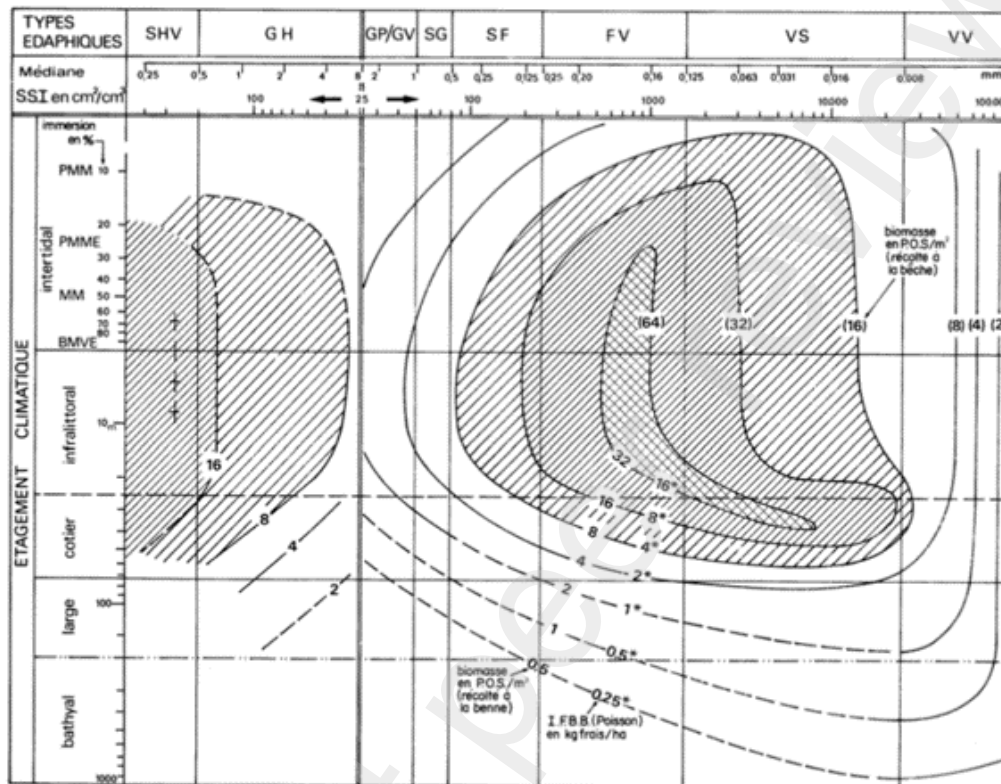
77 into spatial variability in the body condition of benthic-demersal fish predators. Within the Bay of Biscay,
78 benthic-demersal fish communities have been well described (Souissi et al., 2001), and the diets of most
79 species are known (e.g., Rault et al., 2017; Day et al., 2020). With this information, it is possible to
80 characterize the extent to which each species might be dependent on macrobenthic invertebrates.
81 Moreover, thanks to the EVHOE sampling surveys (Laffargue et al., 2020), biometric data are available
82 for multiple benthic-demersal fish species across several years. By analyzing patterns in macrobenthic
83 biomass and the body condition of benthic-demersal fish—and taking into account the diet plasticity of
84 these fish with respect to benthic macrofauna—it might be possible to detect the influence of spatial
85 trends in benthic food resources on higher trophic levels. Such information can then be used to shed
86 light on the broader trophic functioning of continental shelves.

87 The work presented here aimed to (1) describe spatial variability in macrobenthic biomass at the shelf
88 scale in the Bay of Biscay based on data from models, (2) compare these data to the limited field data
89 available, and (3) assess whether macrofaunal biomass data generated by such models exhibit a
90 relationship with the body condition of benthic-demersal fish, and might thus be representative of the
91 underlying availability of food resources.

92 **2. Materials and Methods**

93 **2.1. Macrobenthic biomass indices**

94 **2.1.1. From an empirical biomass model (Chassé and Glémarec, 1976)**



95

96 *Figure 1: Graph model from Chassé and Glémarec (1976). Y-axis corresponds to logged bathymetric*
 97 *depth, and x-axis to granulometry divided into broad substrate categories.*

98

99 The first model used to generate macrobenthic biomass indices was based on a graph of
 100 biomass isopleths created from grab samples in the Bay of Biscay (Chassé and Glémarec, 1976) (Figure
 101 1). Depth data came from depth maps (GEBCO Bathymetric Compilation Group, 2023). This model is
 102 subsequently referred to as the “graph” model.

103 Biomass values were digitized from this graph (Figure 1) for each substrate category (silted
 104 heterogeneous sand (SHV), heterogeneous gravel (GH), clean/muddy gravel (GP/GV), coarse sand
 105 (SG), fine sand (SF), muddy fine sand (FV), sandy mud (VS), and pure mud (VV)), and for each
 106 bathymetric stratum (with a step of 10 m between 0 and 100 m depth, then from 100 to 200 m). Once
 107 rasterized, each cell was assigned a biomass value (in g.m⁻² dry weight (DW)) corresponding to the
 108 lower-bound isopleth. The maximal cell value was 32 g.m⁻² DW, associated with shallow muddy fine

109 sand (FV). Finally, macrobenthic biomass values were assigned to each sub-section (substrate category
110 and bathymetric stratum), corresponding to the averaged biomass value over the proportion of cells.
111 This process provided an average value of macrobenthic biomass for each substrate category and
112 bathymetric stratum.

113 The first substrate map used was the 'Atlas du littoral français: Atlas des fonds meubles du
114 plateau continental du Golfe de Gascogne [Atlas of the French coastline: Atlas of the soft bottoms of the
115 continental shelf of the Bay of Biscay]' obtained from the same study as the graph model described
116 above (Chassé and Glémarec, 1976). The map of biomass indices resulting from this first substrate map
117 is hereafter referred to as the 'Biomass₁₉₇₆ map'. The second substrate map used is more recent than
118 the first (Vasquez et al., 2023) and is based on a more-extensive dataset describing the nature of the
119 seabed. We adapted the substrate categories in this map to correspond to those of the biomass graph
120 model based on a comparative analysis of the two substrate maps (results are in Supplementary
121 Materials 1). The second map of biomass indices is subsequently referred to as the 'Biomass₂₀₂₃ map'.

122 Some approximations were necessary for certain areas (5% of the shelf surface for Biomass₁₉₇₆
123 and Biomass₂₀₂₃ maps) where the substrate x bathymetry intersection was not represented in the graph
124 model, and biomass data were not available. These areas were approximated by another substrate with
125 similar levels of macrobenthic biomass and similar trends along the depth gradient. For the Atlas
126 substrate maps, biomass values for muddy/clean gravel (GP/GV) were approximated by biomass from
127 coarse sand (SG) below 80 meters depth, and biomass values from muddy heterogeneous sand (SHV)
128 were approximated by biomass from muddy fine sand (FV) below 50 meters depth. For the more-recent
129 substrate maps, biomass values of gravel and coarse sand from the graph model were averaged
130 (GP/GV and SG) for the "coarse substrate" category. Descriptions of the substrate categories of the
131 graph model and the two substrate maps are available in Supplementary Materials 2.

132 **2.1.2. From a biogeochemical model (POLCOMS-ERSEM)**

133 The second set of modeled data used to generate a macrobenthic biomass index came from a
134 mechanistic biogeochemical model. The data originated from the outputs of the POLCOMS-ERSEM
135 model, a regional high-resolution coupled hydrodynamic-ecosystem model for low trophic levels, driven
136 by a reanalysis of data from the period 2000–2015 (Kay et al., 2018). POLCOMS-ERSEM links a general
137 ocean circulation model, POLCOMS (the Proudman Oceanographic Laboratory Coastal Ocean

138 Modelling System) and a marine ecosystem model, ERSEM (European Regional Seas Ecosystem
 139 Model; Butenschön et al., 2016). It covers the European shelf seas, with a horizontal resolution of 0.1°
 140 (around 11 km). As we are interested in the biological part of the model, we will refer to it subsequently
 141 as the ERSEM model. In this model, three groups represent the bulk of macrobenthic biomass, and they
 142 were initially calibrated using data estimated by Bryant *et al.* (1995) based on macrobenthic biomass
 143 values in the North Sea. We selected deposit- and suspension-feeding groups as the macrobenthic
 144 components of interest (the only other group, 'meiobenthos', was not considered).

145 Biomass values were summed from all suspension and deposit feeders in ERSEM to create a
 146 macrobenthic biomass index. Macrobenthic biomasses were averaged over the last 10 years (2006–
 147 2015) to minimize potential yearly effects. The macrobenthic biomass index from ERSEM was
 148 expressed in gC/m² and the map of these values is referred to here as the “Biomass_{ERSEM} map”.

149 2. 2. Biological field data

150 2.2.1. Biomass of macrobenthic invertebrates

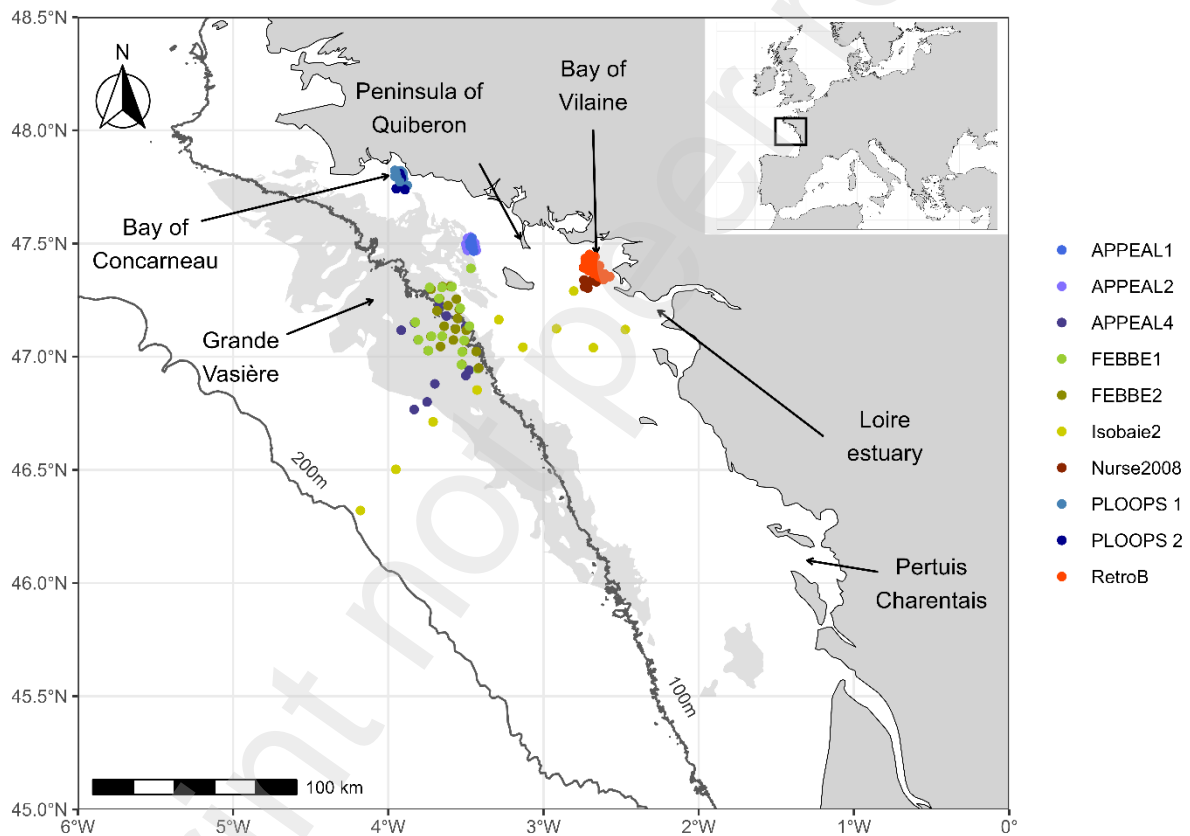
151 Macrobenthic biomass indices from the three biomass maps described above were compared
 152 to field data collected in the circalittoral area (*i.e.*, less than 15 m depth) of the northern part of the shelf
 153 of the Bay of Biscay. Table 1 provides a summary of the various surveys from which data on
 154 macrobenthic biomass were obtained; the spatial distribution of sampled stations (from 2 to 5 grabs per
 155 station) is presented in Figure 2. As seen in this figure, these data are very sparse over both time and
 156 space, and no single survey covers the full extent of the continental shelf.

157 Table 1: Summary of different macrobenthic surveys in which biomass data were collected, with the
 158 gear used, the time of the year, the year sampled, the average bathymetry (and its range), and the
 159 number of stations for each.

Survey	Sampling gear	Time	Bathymetry	N	Reference
RetroB	Van Veen grab	March (2008)	20.1 (15-25.6)	17	(Le Bris, 2008)
Nurse2008	Van Veen grab	August - September (2008)	21.8 (16.3-35.3)	20	(Brind'Amour, 2008)
PLOOPS 1	Van Veen grab	July (2009)	27.6 (23-35)	18	(Dubois, 2010a)
PLOOPS 2	Van Veen grab	February - November (2010)	25.5 (21.3-32.8)	24	(Dubois, 2010b)
Isobaie 2	Van Veen grab	June (2010)	77.3 (18.9-154)	11	(Le Bris, 2010)
FEBBE 1	Day grab	May - August (2013)	101.3 (78-113)	18	(Laffargue, 2013a)
FEBBE 2	Day grab	August (2013)	101.9 (91-113)	23	(Laffargue, 2013b)
APPEAL1	Hamon grab	May (2018)	60.7 (53-74)	15	(Le Loc'h and Grall, 2018a)
APPEAL 2	Hamon grab	August (2018)	59.2 (52-73)	15	(Le Loc'h and Grall, 2018b)
APPEAL 4	Hamon grab	September (2019)	109.5 (98.4-125.1)	12	(Le Loc'h and Grall, 2019)

160

161 RetroB and Nurse2008 were two surveys performed in a coastal bay (Bay of Vilaine)
 162 (Brind'Amour, 2008; Le Bris, 2008), in a shallow circalittoral area under the terrigenous influence.
 163 PLOOPS 1 and 2 surveyed a coastal area in the Bay of Concarneau (Dubois, 2010a; Dubois, 2010b),
 164 which, although it also features a shallow circalittoral fringe, has less terrigenous influence compared to
 165 the Bay of Vilaine. APPEAL 1 and 2 focused on the deeper limit of the shallow circalittoral fringe, to the
 166 south of the island of Groix (Le Loc'h and Grall, 2018a; Le Loc'h and Grall, 2018b). APPEAL 4 and
 167 FEBBE 1 and 2 surveyed a deep circalittoral muddy bank, the so-called "Grande Vasière" (Laffargue,
 168 2013a; Laffargue, 2013b; Le Loc'h and Grall, 2019). Finally, Isobaie 2 covered a coastal-to-offshore
 169 transect from the Loire estuary and Bay of Vilaine towards the shelf break (Le Bris, 2010).



170

171 *Figure 2: Locations of macrobenthic field observation stations on the northern shelf of the Bay of Biscay.*
 172 *Different surveys are represented with different colors. The light gray shaded area is the mid-shelf mud*
 173 *belt known as the "Grande Vasière".*

174 Each survey counted taxa down to the lowest taxonomic level, and biomass was measured for
 175 most of the taxa, sampled stations, and studies. When individual mass was not available, it was
 176 approximated using values from the closest phylogenetic relative from the same station or from a
 177 neighboring station of the same survey. Biomass values in wet weight were converted into ash-free dry

178 weight using Brey's conversion factors (www.thomas-brey.de/science/virtualhandbook). For each
179 station, observed macrobenthic biomass was the average of the values obtained from two to five
180 replicates.

181 **2.2.2. Data on individual benthic-demersal fish**

182 Individual biometric data (total length and mass) from autumnal EVHOE surveys (between 2008
183 and 2022, onboard *Thalassa R/V*) were used to assess the body condition of a limited selection of
184 benthic-demersal fish species. Body condition is ultimately a reflection of a fish's habitat quality, and
185 consequently also of food resource availability (Cavraro et al., 2019; Karlson et al., 2018; Liao et al.,
186 1995; Schloesser and Fabrizio, 2019). We examined most of the benthivorous species for which
187 sufficient data were available across the continental shelf (Supplementary Materials Figure SM4 and
188 SM5). Four demersal species were considered: whiting (*Merlangius merlangus*), striped red mullet
189 (*Mullus surmuletus*), poor cod (*Trisopterus minutus*), and pout (*Trisopterus luscus*). Four benthic taxa
190 were also considered: scadfish (*Arnoglossus* spp.), small-spotted catshark (*Scyliorhinus canicula*),
191 common sole (*Solea solea*), and thickback sole (*Microchirus variegatus*). *Arnoglossus* spp. includes
192 both *A. laterna* and *A. imperialis*, which are assumed to have a similar diet (Castro et al., 2013), and the
193 combination of the two made it possible to cover a wide coastal-to-offshore gradient.

194 **2.3. Data analysis**

195 **2.3.1. Comparison of macrobenthic biomass indices from models**

196 Once we had generated the maps of the three macrobenthic biomass indices, we compared the
197 spatial patterns presented. Each map was standardized and gridded with the 0.1° x 0.1° ERSEM grid,
198 and each grid cell was assigned an average biomass index value (weighted by the surface area of each
199 biomass value within the grid cell). Biomass_{ERSEM}, Biomass₁₉₇₆, and Biomass₂₀₂₃ were then compared
200 using Spearman correlations. Specifically, for a given cell, a buffer area of 5 cells was considered
201 (resulting in a 25-cell window) and Spearman correlations were computed for the values of each
202 biomass map in this window, allowing us to highlight potential differences in spatial trends between the
203 different maps. Negative values meant that the two maps in question depicted opposite trends in
204 macrobenthic biomass. All analyses were conducted using R 4.3.1 (R core team, 2023); maps were
205 processed using the raster and sf packages (Hijmans, 2023; Pebesma, 2018).

206 **2.3.2. Comparison between field data on macrobenthic biomass and biomass indices**
207 **from models**

208 Macrobenthic biomass indices from the three maps generated here were compared to values
209 of macrobenthic biomass from field datasets. For this, the nearest macrobenthic biomass values from
210 each of the three maps were assigned to each field station sampled, and these values were averaged
211 within a 500-m buffer surrounding the station. Values from biomass index maps and field values were
212 log-transformed and normalized so that the final data ranged between 0 and 1. Then, Spearman
213 correlations were calculated between macrobenthic biomass values from field data and indices from
214 models.

215 **2.3.3. Relationship between body condition and macrobenthic biomass indices**

216 Fish body condition was assessed using the body condition factor developed by Le Cren (1951),
217 which represents 'the deviation of an individual from the average weight for length' in a given population.
218 Le Cren's condition factor, K_n , compensates for allometric changes, enabling comparisons of body
219 condition between small and large individuals. Indeed, the response of body condition to macrobenthic
220 resource availability may vary in a size-dependent manner due to trophic shifts and diet plasticity.

221 For each species, log length-mass relationships (LMR) were fitted using individual biometric
222 data. Observations with a Cook's distance greater than $4/n$ (n = number of observations) were
223 considered outliers and removed (Altman and Krzywinski, 2016). For each species, homogeneity of
224 variance and the normal distribution of residuals were checked visually.

225 K_n is the observed individual mass divided by the predicted mass according to each species'
226 LMR. To take into account ontogenic variations, individuals were split into two size groups, to reflect the
227 trophic size thresholds reported in the literature for six of the fish species (Table 2).

228 Finally, we created mixed-effect linear models to assess the relationship between the body
229 condition factor and the macrobenthic biomass indices. One model was computed for each of the eight
230 fish taxa and the three macrobenthic biomass index maps (Biomass₁₉₇₆, Biomass₂₀₂₃, and
231 Biomass_{ERSEM}), and fitted using the lme4 R package (Bates et al., 2015). Models were computed with
232 station as a random effect to account for intra-station correlations (Zuur et al., 2009) and also included
233 a size category effect (*i.e.*, Small or Large), with the exception of the models for *Arnoglossus* spp. and

234 *Microchirus variegatus*. Each station was assigned the average value of macrobenthic biomass within
 235 a 5000-m buffer around its location. The sensitivity of results to this buffer was explored, and no major
 236 differences were observed when comparing results from 1-km to 50-km buffers. Macrobenthic biomass
 237 indices were scaled to allow the comparison of their respective effects on K_n . Chi-squared tests were
 238 used to evaluate these results against the null hypothesis (*i.e.*, a model without a biomass effect). During
 239 model evaluation, mixed-effect linear models were refitted using maximum likelihood, and only
 240 significant models (p -value < 0.05) were kept. Additionally, the variance explained by selected mixed-
 241 effect linear models was computed using conditional R-squared and marginal R-squared values;
 242 conditional R-squared included random and fixed effects of the model, while marginal R-squared
 243 corresponded to the variance explained only by the fixed effect (Zuur et al., 2009).

244 Since the spatial extent of the biomass maps varied, the amount of data per species and size
 245 class available for the mixed-effect linear models also differed. The quantity of data used for each mixed-
 246 effect linear model and each macrobenthic biomass model is provided in Table SM6.

247 Table 2: Size thresholds used to account for ontogenic shifts in different fish species.

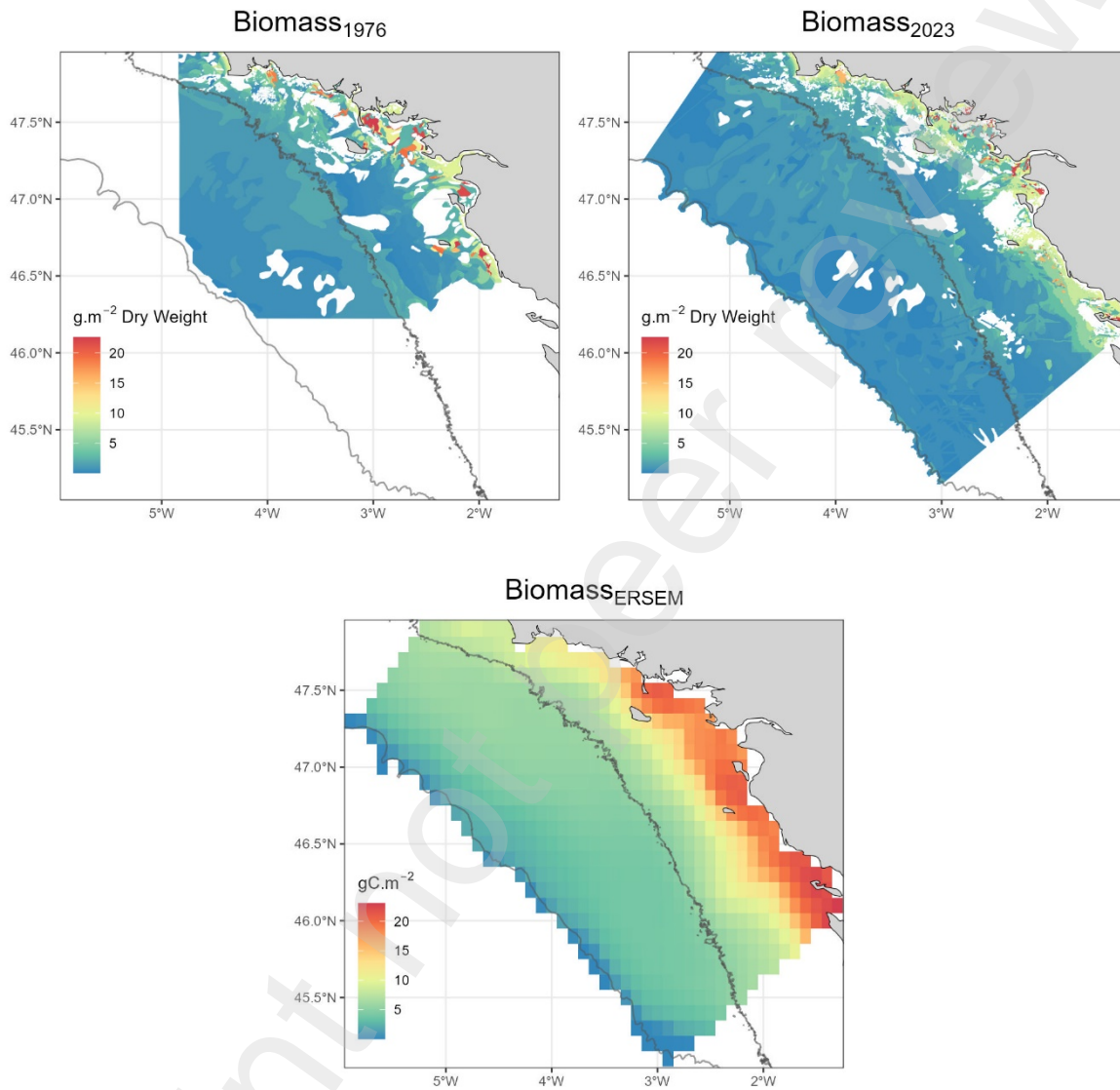
Species	Size shift	Trophic shift	Reference
<i>Arnoglossus spp.</i>	-		(Schückel et al., 2011)
<i>Merlangius merlangus</i>	20	Shift from benthic invertebrates to fish.	(Hislop et al., 1991)
<i>Microchirus variegatus</i>	-		(Amezcuca et al., 2003)
<i>Mullus surmuletus</i>	18	Shift from benthic invertebrates to shrimp, ophiurids, and polychaetes.	(Bautista-Vega et al., 2008)
<i>Scyliorhinus canicula</i>	22	Shift from small invertebrates to larger decapods, cephalopods, and fish.	(Šantić et al., 2012)
<i>Solea solea</i>	30	Shift toward epibenthic decapods and higher trophic level.	(Fanelli et al., 2022)
<i>Trisopterus luscus</i>	25	Shift from benthic invertebrates towards shrimp and fish.	(Armstrong, 1982)
<i>Trisopterus minutus</i>	17	Shift from small crustaceans to larger decapods and fish.	(Armstrong, 1982)

248

249 **3. Results**

250 **3.1. Maps of macrobenthic biomass indices**

251



252

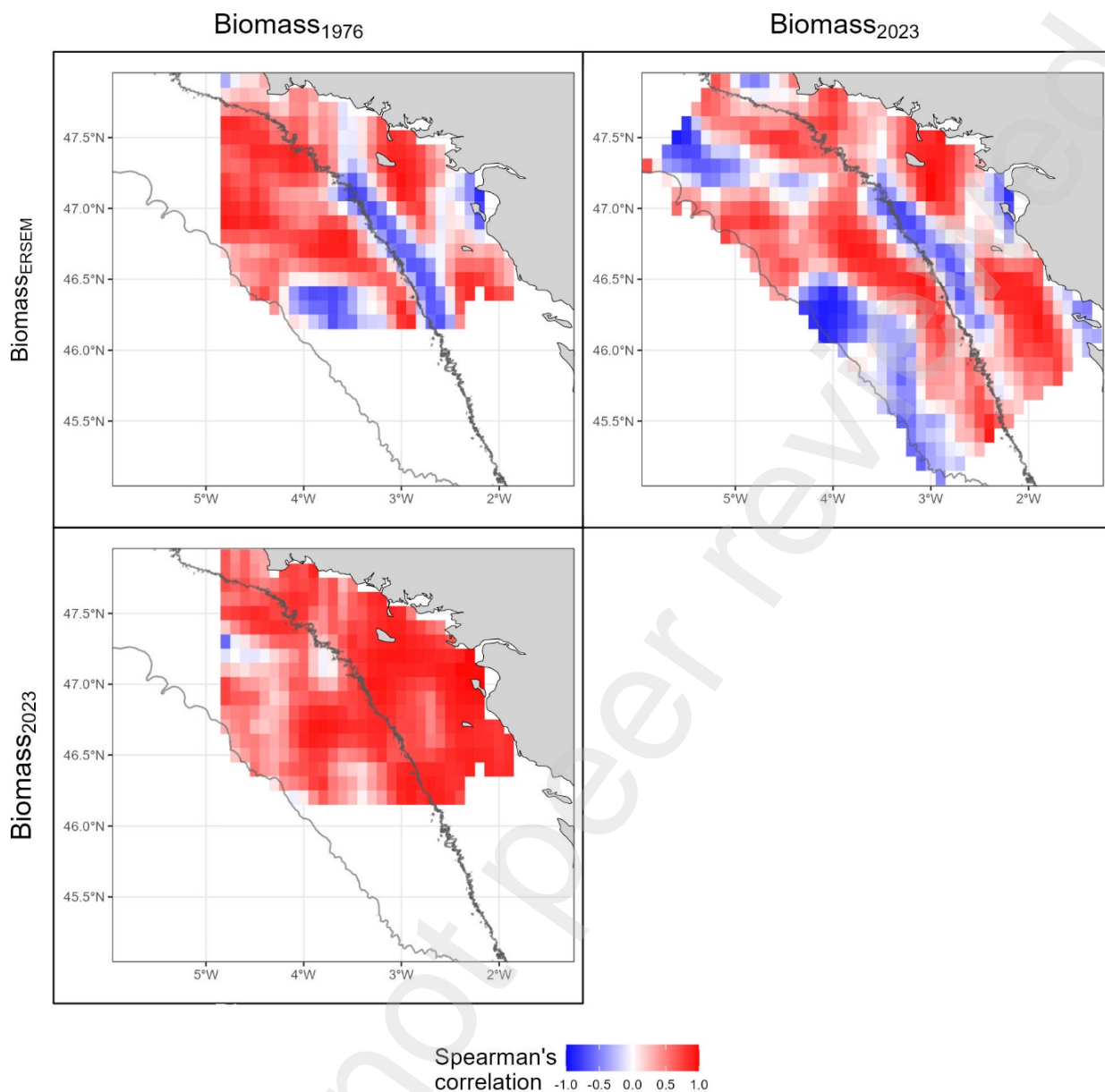
253 *Figure 3: Maps of macrobenthic biomass indices obtained from the graph and ERSEM models. White*
254 *areas in the Biomass₁₉₇₆ and Biomass₂₀₂₃ maps correspond to hard bottom substrate, where soft bottom*
255 *macrobenthic biomass could not be assessed. Gray lines represent the 100- and 200-meter isobaths.*

256

257 The Biomass₁₉₇₆ and Biomass₂₀₂₃ maps highlighted high values of macrobenthic biomass along
258 the coast, in concentrated areas characterized by shallow patches of mud, sandy mud, and muddy sand

259 substrate. Instead, index values from the Biomass_{ERSEM} map were higher along a coastal fringe ranging
260 from the Pertuis-Charentais to the peninsula of Quiberon (Figure 3).

261 The Biomass_{ERSEM} map depicts a decreasing gradient in biomass towards the shelf break, inversely
262 related to water depth, while the Biomass₁₉₇₆ and Biomass₂₀₂₃ maps highlight patches of substrate at
263 moderate depths that support higher macrobenthic biomass. Overall, the Biomass₁₉₇₆ and Biomass₂₀₂₃
264 maps were highly correlated (Spearman correlation = 83.09%), while the Biomass_{ERSEM} map exhibited
265 a weaker correlation with the two others (49.82% and 62.84%, respectively). The most substantial
266 differences were noted between the Biomass₁₉₇₆ and Biomass_{ERSEM} maps; patches corresponding to
267 certain habitats (*e.g.*, the large mud belt in the central part of the shelf, or at the edge of the continental
268 shelf) exhibited opposing trends in macrobenthic biomass between these two maps (Figure 4).



269

270 *Figure 4: Maps of local Spearman correlations, with blue representing negative correlations and red*
 271 *positive correlations. Gray lines represent the 100- and 200-meter isobaths.*

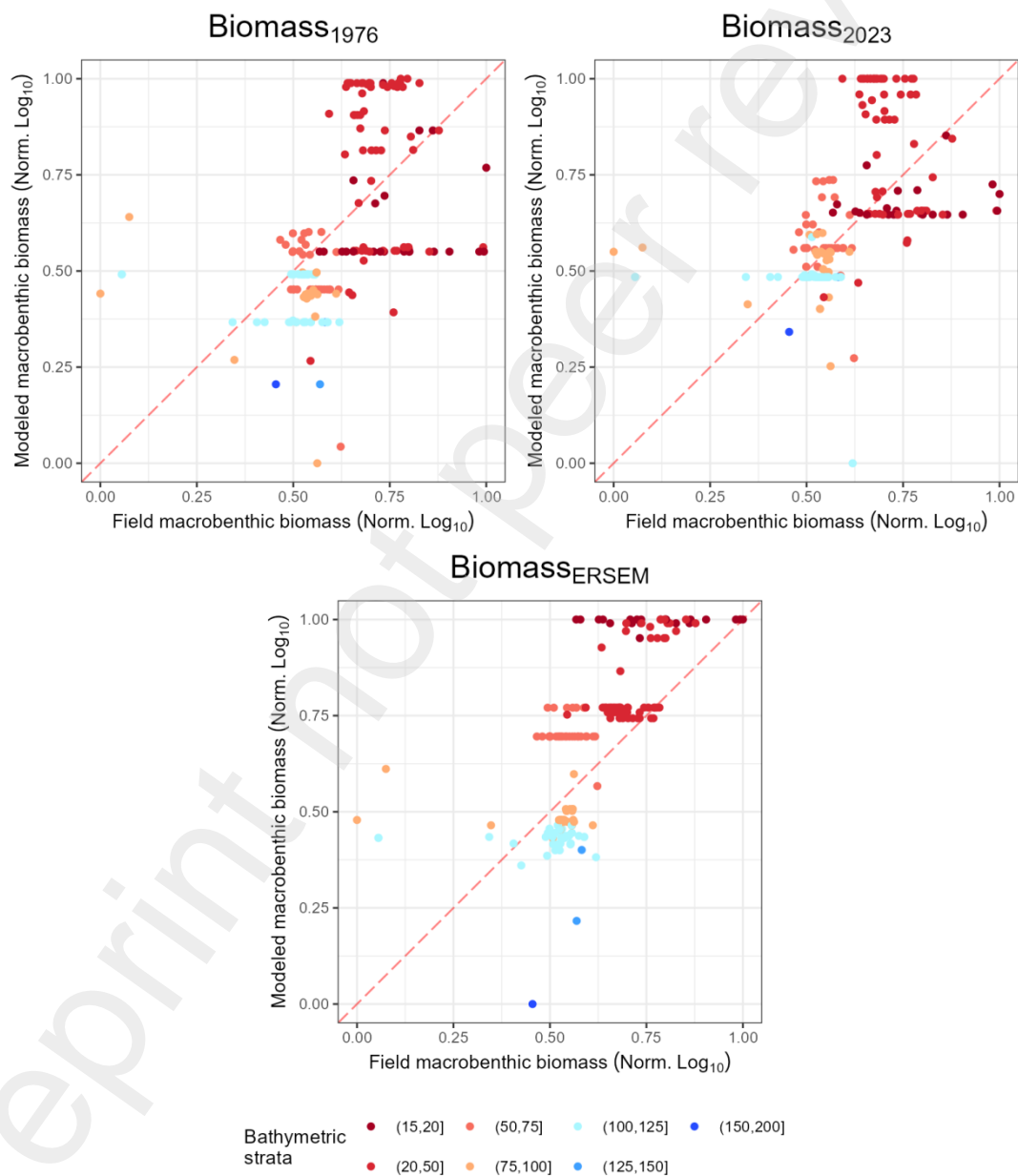
272

273 **3.2. Biomass indices from models versus field biomass data**

274 Despite differences in absolute trends, positive Spearman correlations were detected between
 275 the three indices of macrobenthic biomass and field data on macrobenthic biomass (60.4%, 66.9%, and
 276 77.5% for Biomass₁₉₇₆, Biomass₂₀₂₃, and Biomass_{ERSEM}, respectively; Figure 5). Based on the ERSEM
 277 model, the highest level of biomass was predicted for stations located at 15–20 m depth. Instead, the
 278 graph model (Biomass₁₉₇₆ and Biomass₂₀₂₃) estimated the highest levels of biomass at a depth of 20-50

279 m, and similar, lower, levels between stations at 15–20 m and 50–75 m. Most of the stations that were
 280 estimated to have high biomass levels (from Biomass₁₉₇₆ and Biomass₂₀₂₃) were sampled as part of the
 281 PLOOPS surveys (Figure SM7). The bathymetric gradient previously noted in the Biomass_{ERSEM} index
 282 is also evident in Figure 5, as stations tended to aggregate along the y-axis according to their
 283 bathymetry. This pattern was less marked for the Biomass₁₉₇₆ and Biomass₂₀₂₃ indices, which generated
 284 similar estimates of biomass at depths of 50–75 m and 75–100 m.

285



286

287 Figure 5: Modeled macrobenthic biomass indices versus field data on macrobenthic biomass. Stations
 288 are colored according to their bathymetric range, with red shades for shallower depths and blue for
 289 deeper ones. The red dashed line corresponds to the isoline.

290

291 3.3. Relationship between body condition and macrobenthic biomass indices

292 Of the numerous mixed-effect linear models we constructed to test the effect of the
 293 macrobenthic biomass indices as predictors of body condition in various fish species, 15 detected
 294 significant effects, *i.e.*, a macrobenthic biomass index explained significantly more variance than the null
 295 model (Table 3). No such models were found for *Trisopterus minutus* and *Scyliorhinus canicula*, and
 296 only one significant model was obtained for *Microchirus variegatus* and for *Merlangius merlangus*.
 297 Instead, significant positive relationships were found between the three macrobenthic biomass indices
 298 and body condition factors for the species *Arnoglossus spp.*, *Mullus surmuletus*, *Solea solea*, and
 299 *Trisopterus luscus*. The level of variance explained remained globally low, with the maximum observed
 300 for the relationship between body condition in *Mullus surmuletus* and the Biomass₁₉₇₆ index (14.7%)
 301 (Table 3). On average, *Mullus surmuletus* and *Arnoglossus spp.* were the two taxa with the highest
 302 amount of variance explained by macrobenthic biomass indices.

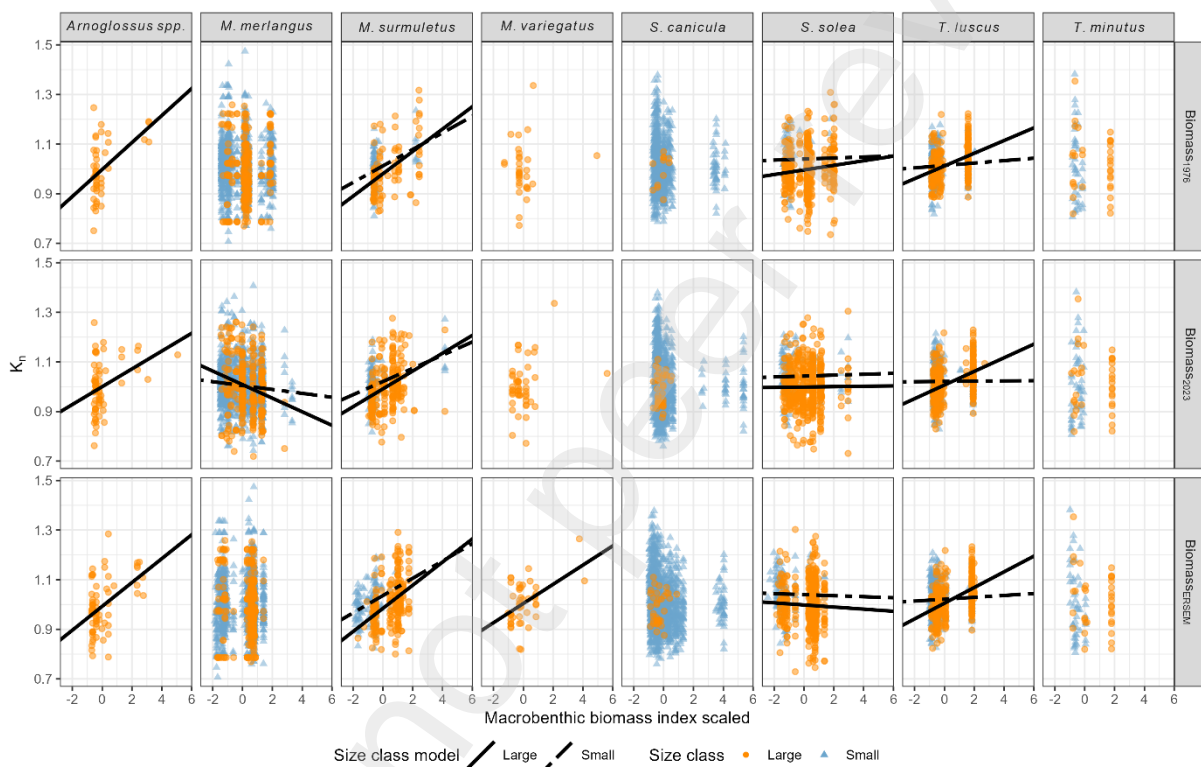
303 Table 3: Summary of mixed-effect linear models that identified a significant relationship between
 304 macrobenthic biomass indices and body condition factors of fish. Chi2 and p-value correspond to the
 305 test of the model against a null model including only an intercept and the random effect of station. R2m
 306 is the marginal R-squared value and R2c is the conditional R-squared value.

Macrobenthic index	Species	R2m	R2c	Chi2	p-value
Biomass ₁₉₇₆	<i>Arnoglossus spp.</i>	0.143	0.419	5.4	2.01e-02
	<i>Mullus surmuletus</i>	0.147	0.327	14.94	1.87e-03
	<i>Solea solea</i>	0.038	0.197	18.46	3.53e-04
	<i>Trisopterus luscus</i>	0.066	0.183	8.11	4.38e-02
Biomass ₂₀₂₃	<i>Arnoglossus spp.</i>	0.073	0.383	4.01	4.52e-02
	<i>Merlangius merlangus</i>	0.014	0.183	9.22	2.65e-02
	<i>Mullus surmuletus</i>	0.085	0.313	15.54	1.41e-03
	<i>Solea solea</i>	0.034	0.18	19.84	1.83e-04
	<i>Trisopterus luscus</i>	0.072	0.229	20.18	1.56e-04
Biomass _{ERSEM}	<i>Arnoglossus spp.</i>	0.126	0.43	5.87	1.54e-02
	<i>Microchirus variegatus</i>	0.131	0.464	5.33	2.10e-02
	<i>Mullus surmuletus</i>	0.1	0.301	23.67	2.93e-05

<i>Solea solea</i>	0.038	0.184	20.22	1.53e-04
<i>Trisopterus luscus</i>	0.085	0.238	22.64	4.80e-05

307

308 In all taxa in which a significant relationship was detected between body condition and macrobenthic
 309 biomass, the relationship was positive; the only exception to this was found in *M. merlangus*.
 310 Additionally, these relationships were stronger (steeper slope) for smaller-sized individuals, although
 311 this pattern was identified for large individuals of *Mullus surmuletus* as well.



312

313 *Figure 6: Significant linear mixed-effect models selected. Data used to fit models are shown here;*
 314 *orange dots correspond to small individuals and blue triangles to larger ones.*

315

316

317 The only species for which K_n exhibited a steep negative relationship with macrobenthic biomass was
 318 *Merlangius merlangus*. For *Solea solea*, instead, larger individuals seemed to show higher values of K_n ,
 319 with only a very weak (positive or negative depending on the biomass index) relationship with
 320 macrobenthic biomass indices.

321 4. Discussion

322 The northern part of the shelf of the Bay of Biscay is a particularly productive ecosystem,
323 supporting both pelagic and benthic trophic pathways (Cresson et al., 2020) that provide essential
324 resources for fish species. One such resource is the macrobenthos; these organisms are a key food
325 source for benthic-demersal fish, which tend to be opportunists that will eat whatever benthic prey is
326 available (Day et al., 2019; Rault et al., 2017). However, spatial variability in macrobenthic biomass on
327 this shelf remains largely unexplored. To date, quantitative data on macrobenthic biomass in the Bay of
328 Biscay are limited to very coastal areas (e.g., Dutertre et al., 2013) or specific habitats (e.g., muddy
329 areas like the Grande Vasière; (Le Loc'h et al., 2008). The benthic characteristics of these areas have
330 been extrapolated to the entire shelf through ecosystem modeling (Lassalle et al., 2011). The present
331 study aims to fill this gap by analyzing the spatial distribution of macrobenthic biomass over the whole
332 northern shelf of the Bay of Biscay and evaluating the relationship between variations in this biomass
333 and the fish that feed (to a greater or lesser degree) on the macrobenthos. The lack of field data on
334 macrofaunal biomass in much of the study area prompted us to explore and use existing models, of
335 which two were particularly relevant to our objective and the marine region we were studying.

336 The empirical “graph model” from Chassé and Glémarec (1976) is based on depth and sediment
337 typology, with the assumption that hydro-sedimentary characteristics drive ecological processes and
338 features of macrobenthic communities (Glémarec, 1969; McArthur et al., 2010; Reiss et al., 2015). The
339 graph model was defined on the basis of a limited number of sediment classes, reflecting the substrate
340 distribution presented in the “Atlas des fonds meubles du plateau continental Nord Gascogne” [Atlas of
341 the French coastline: Atlas of the soft bottoms of the continental shelf of the Bay of Biscay] (Chassé and
342 Glémarec, 1976). This modeling strategy is comparable to the habitat suitability modeling framework
343 adopted by Degraer et al. (2008), since the map involved an initial biophysical dataset and spatial
344 interpolation from this dataset with physical data maps.

345 In the ERSEM model, which is part of the POLCOMS-ERSEM biophysical model, macrobenthic
346 biomass of suspension and deposit feeders is the direct result of flows from ecological processes
347 (primary production, organic matter sedimentation) that supply the seafloor. Benthic-pelagic coupling
348 models like the ERSEM model have already demonstrated their ability to accurately represent
349 macrobenthic biomass at a small scale (Ehrnsten et al., 2019). This model also incorporates other

350 processes, such as organic matter ingestion or bioturbation (Butenschön et al., 2016)—but not the
351 remobilization of buried organic matter (Butenschön et al., 2016)—that could boost macrobenthic
352 biomass (Qin et al., 2010) and benefit the benthos during periods of low input (Zhang et al., 2019).
353 However, the ERSEM model is only based on muddy sediments and, unlike the graph model, does not
354 account for spatial variability in substrate types, despite the critical role these characteristics play in the
355 modeled processes and in determining benthic invertebrate biomass. Indeed, the nature of a substrate
356 reflects numerous features and processes (*e.g.*, permeability, deposition, resuspension, organic
357 content, among others) (Chen et al., 2018; Idier et al., 2010; Pace et al., 2021) that can influence
358 macrobenthic characteristics and biomass (Ehrnsten et al., 2019; Pearson and Rosenberg, 1978).

359 The graph and ERSEM models reproduced biomass gradients that were largely similar to each
360 other, particularly in the overall decrease from the coast to the shelf break and the presence of
361 heterogeneous coastal zones with high biomass. This gradient is indicative of a significant terrigenous
362 influence, one whose intensity increases with proximity to river outlets (Loire and Vilaine estuaries),
363 particularly in the southeastern region of the study area. However, there were substantial differences
364 between the two types of models. The two maps derived from the graph model showed discontinuities
365 in this biomass gradient, with distinct patches of high biomass values, particularly in the muddiest zone
366 (the Grande Vasière). With the graph model, the use of the most recent substrate map only marginally
367 changed the distribution of biomass; this was unsurprising given that these maps largely reproduce
368 substrate data from previous versions and retain high local uncertainties due to their extremely
369 heterogeneous spatial sampling coverage and limited sedimentary field data (Kaskela et al., 2019;
370 Pierrejean et al., 2022). Instead, the biomass distribution provided by the ERSEM model was much less
371 patchy, illustrating the more continuous nature of the spatial distribution of the variables used to estimate
372 biomass, especially because this model does not take into account sedimentary substrate features.

373 Based on an exhaustive census of surveys and research projects carried out over the last
374 decade, we gathered all available field data on spatial variability in macrobenthic biomass in the study
375 area. A preliminary analysis of the data highlighted not only spatial gaps (especially between 120 and
376 200 m) but also heterogeneity in the sampling gear used (3 types) and in the years (10 years from 2008
377 to 2019) and months/seasons (from March to November) in which samples were collected. Keeping in
378 mind these limitations, when these data were standardized and examined at a broad scale, they seemed
379 to describe a depth gradient roughly comparable to those we estimated from models (Spearman

380 correlations ranging from 60% to 80%). Even the limited amount of field data we were able to find is
381 useful in understanding the strengths or deficiencies of the models. For example, when comparing
382 coastal areas, the ERSEM model seemed to better reflect the reality of the observed biomass difference,
383 which was lower in the Bay of Concarneau (PLOOPS surveys) than in the Bay of Vilaine (RetroB and
384 Nurse2008 surveys). This difference was reversed in the graph model, which seemed to underestimate
385 macrobenthic biomass in pure muddy substrates such as those found in the Bay of Vilaine (Le Bris and
386 Glémarec, 1995). This may reflect the fact that terrigenous influences, which are known to increase
387 benthic biomass (Deubel et al., 2003; Escobar-Briones and Soto, 1997; Zuschin and Stachowitsch,
388 2009), were not taken into account in the graph model, which only considered depth and sediment type.
389 This point was discussed by Dutertre *et al.* (2013), who explained that in the shallow part of the Bay of
390 Biscay, although 26% of macrobenthic diversity patterns could be explained by substrate,
391 hydrodynamics, and depth, the inclusion of parameters quantifying riverine influence (Vilaine and Loire)
392 made it possible to explain an additional 16%.

393 For both types of models, there is a notable deficiency at the continental shelf edge. The
394 absence of a peak in macrobenthic biomass at the shelf edge seems to indicate that the two models
395 ignore the hydrological context of the shelf break, where biological production is stimulated by upwelling
396 (Simpson and Sharples, 2012; Vandromme et al., 2014). Although limited field data were available in
397 this area, some of the deepest field observations could indicate the presence of a peak; such a pattern
398 would be consistent with estimates made by Le Loc'h *et al.* (2008) at three sampling stations in the slope
399 area, which they compared to the highly productive mud zone in the middle of the continental shelf.

400 By analyzing the relationship between fish body condition and macrobenthic biomass indices,
401 our aim was to explore the impact of the distribution of food resources on the shelf as indicated indirectly
402 by the macrobenthic component. In our study, the relationship between macrobenthic biomass indices
403 and body condition factor (K_n) was significant and positive for four of the eight benthic-demersal fish
404 species tested. These relationships were similar for all models of macrobenthic biomass and for most
405 of the fish species examined, which emphasizes the importance of the coastal-to-offshore gradient in
406 the spatial distribution of macrobenthic food resources. It also suggests bottom-up processes in which
407 food availability may be a determining factor, as seen in other contexts (Brosset et al., 2015; Laurel et
408 al., 2001; Porath and Peters, 1997).

409 In many cases, the presence or absence of significant relationships can be explained by the
410 trophic or life-history characteristics of the species analyzed. Among the different species studied,
411 whiting (*Merlangius merlangus*), poor cod (*Trisopterus minutus*), and small-spotted catshark
412 (*Scyliorhinus canicula*) exhibited a negative or non-existent relationship between body condition and
413 biomass indices. For whiting, this could be explained by the fact that the diet of small individuals (less
414 than 22 cm) is both pelagic and benthic, while that of larger individuals is also based on pelagic and
415 demersal fishes (Day et al., 2019). This feeding characteristic is shared by the poor cod, which has a
416 very generalist diet featuring macrobenthic, suprabenthic, and pelagic prey, including fish at larger sizes
417 (Armstrong, 1982). The small-spotted catshark is also thought to feed on pelagic resources such as
418 euphausiids (Rodríguez-Cabello et al., 2007), which are often found near the continental slope of the
419 Bay of Biscay (Peña et al., 2019), where the fish in our study were mainly found. For these species, the
420 absence of significant relationships with macrobenthic biomass may reflect dietary compensation with
421 pelagic prey when benthic food resources are less available.

422 Compared to the other flatfish studied, the common sole (*Solea solea*) did not exhibit a strong
423 positive relationship between body condition and macrobenthic biomass indices, even though it is mostly
424 benthivorous (Lagardère, 1987; Rault et al., 2017). For small sole individuals, whose distribution is more
425 coastal than that of large individuals, it is difficult to find an explanation for this weak relationship. For
426 large individuals, which are mainly found further offshore (Figure SM5), the relatively high body condition
427 scores in an area of poorer macrobenthic biomass may be related to the fact that these individuals have
428 accumulated reserves in more coastal areas during the summer period (Rijnsdorp, 1990), before
429 migrating offshore in the autumn (where they were sampled) to reproduce a few months later (Le Bec,
430 1983). This may not be the case for the other fish that did show a relationship between their body
431 condition and macrobenthic biomass, such as *Arnoglossus* spp. and *M. surmuletus*, which are known
432 to reproduce later than the common sole (Gibson and Ezzi, 1980; N'Da and Déniel, 1993).

433 In the case of pout (*Trisopterus luscus*), only the smaller individuals demonstrated a strong
434 positive relationship between body condition and macrobenthic biomass. The small individuals of this
435 species are known to feed mainly on macrobenthic and suprabenthic invertebrates (Castro et al., 2013),
436 while the diet of larger individuals includes fish (Armstrong, 1982). Scalfishes (*Arnoglossus* spp.) and
437 the two age classes of striped red mullet (*M. surmuletus*) also exhibited strong relationships between
438 body condition and macrobenthic biomass indices. Scalfishes feed mainly on suprabenthic

439 invertebrates (Castro et al., 2013), but also on macrofauna and even benthic fish (Déniel, 1981). Striped
440 red mullet feed on epibenthic crustaceans (e.g., Galatheidae and Portunidae) but mainly rely on more
441 infaunal prey such as bivalves or polychaetes (Pavičić et al., 2018; Serrano et al., 2003). Unlike these
442 other species, thickback sole (*M. variegatus*) demonstrated a relationship only between its body
443 condition and the macrobenthic biomass index from the ERSEM map. Its diet relies heavily on benthic
444 macroinvertebrates (Amezcuca et al., 2003; King and Fives, 1990) and it is difficult to explain why the
445 relationship was not established using the data from the other two maps.

446 With the diets of these species in mind, it seems justifiable to assume that the macrobenthic
447 biomass maps also represent a wider range of benthic prey, such as suprabenthic prey which are less
448 effectively sampled by grabs (Sorbe, 1981). The various relationships observed between fish body
449 condition and biomass maps illustrate both differences among fish species in their dependence on
450 benthic resources as well as variability in the availability of such resources. Certain areas (e.g., coastal
451 habitats or mudflats like the Grande Vasière) offer better feeding conditions for benthic-feeding fishes.
452 In such areas, competition between benthic feeders is reduced through processes such as individual
453 specialization (Sánchez-Hernández et al., 2021). Areas with scarcer benthic resources, such as deeper
454 zones (e.g., in the vicinity of the shelf edge), may instead experience heightened intra- and interspecies
455 competition (Holbrook and Schmitt, 1989). This could drive adaptive strategies such as shifts to (i) prey
456 with lower energy content, with consequences for fish growth and body condition (Cormon et al., 2016;
457 Hiddink et al., 2016; Kamimura et al., 2021) and/or (ii) prey at higher trophic levels as suggested by the
458 isotope study of Schaal et al. (2016). This highlights the trophic plasticity of fish with respect to conditions
459 of resource availability or competition (Pelage et al., 2022). Our study supports the idea that demersal
460 fishes generally depend on trophic resources at spatial scales that are smaller than that of the
461 continental shelf, a hypothesis that has already been corroborated by different approaches (e.g.,
462 Chouvelon et al., 2012). Our body condition results are also consistent with the trends reported by
463 Schaal et al. (2016) regarding the trophic levels of demersal fishes along the coastal-to-offshore isotopic
464 gradient, which were characterized by a trophic shift that those authors hypothesized to be due to lower
465 prey abundance offshore.

466

467 **5. Conclusion**

468 By providing visual representations of the spatial distribution of benthic resource availability, the
469 macrobenthic biomass maps analyzed here could be valuable tools in the study of spatial variability in
470 trophic networks, benthic-pelagic coupling, and matter fluxes on the continental shelf. The two models
471 we used to estimate macrobenthic biomass had different strengths and limitations based on the different
472 modeling assumptions employed. Nevertheless, both models, which are based on different ecological
473 hypotheses, revealed similar coastal-to-offshore distribution trends, with notable differences in the mid-
474 shelf and near-coastal areas. Unfortunately, few of Europe's continental shelves (e.g., in the North Sea;
475 Reiss et al., 2010) have been sampled thoroughly enough to effectively reveal benthic biomass
476 gradients on a large spatial scale. These data are crucial for understanding certain processes affecting
477 marine populations or, more recently, for the development of ecosystem models (e.g., Lassalle et al.,
478 2011; Corrales et al., 2022; Lopez De Gamiz-Zearra et al., 2023), especially in deeper areas where
479 macrobenthic samples are limited (e.g., beyond the Grande Vasière in the Bay of Biscay).

480 To better understand the functioning and status of fish populations, our study highlighted the
481 importance of recognizing spatial variability in the macrobenthic resources on which these fish depend.
482 The coastal-to-offshore gradient in macrobenthic biomass, and its relationship with body condition in
483 certain benthic-demersal fish, raises an important question about the viability of deeper populations. This
484 question is all the more crucial in the context of climate change: for example, deepening mechanisms
485 have been clearly demonstrated in benthic-demersal fish on the continental shelves of the northeast
486 Atlantic (e.g., Dulvy et al., 2008) and their impact on the populations of the species concerned has yet
487 to be fully assessed.

488

489 **Acknowledgements:**

490 The authors wish to thank the crew of each survey, as well as the technicians involved in the sampling
491 at sea during surveys and in the laboratory. The authors also wish to thank Stanislas Dubois, François
492 Le Loc'h, and Anik Brind'Amour for providing access to the data from the surveys they directed. We
493 thank Plymouth Marine Laboratory and Susan Kay for providing the POLCOMS-ERSEM projections.
494 This work was supported by a PhD grant from the project Bentroph, which was co-funded by the Brittany
495 region and IFREMER.
496

497 **References**

- 498 Altman, N., Krzywinski, M., 2016. Analyzing outliers: influential or nuisance? *Nature*
499 *Methods* 13, 281–282. <https://doi.org/10.1038/nmeth.3812>
- 500 Amezcua, F., Nash, R., Veale, L., 2003. Feeding habits of the Order Pleuronectiformes
501 and its relation to the sediment type in the north Irish Sea. *Journal of the Marine*
502 *Biological Association of the UK* 83, 593–601.
503 <https://doi.org/10.1017/S0025315403007525h>
- 504 Armstrong, M.J., 1982. The predator-prey relationships of Irish Sea poor-cod
505 (*Trisopterus minutus* L.), pouting (*Trisopterus luscus* L.) and cod (*Gadus*
506 *morhua* L.). *ICES Journal of Marine Science* 40, 135–152.
507 <https://doi.org/10.1093/icesjms/40.2.135>
- 508 Bates, D., Mächler, M., Bolker, B., Walker, S., 2015. Fitting Linear Mixed-Effects
509 Models Using lme4. *J. Stat. Soft.* 67. <https://doi.org/10.18637/jss.v067.i01>
- 510 Bautista-Vega, A.A., Letourneur, Y., Harmelin-Vivien, M., Salen-Picard, C., 2008.
511 Difference in diet and size-related trophic level in two sympatric fish species,
512 the red mullets *Mullus barbatus* and *Mullus surmuletus*, in the Gulf of Lions
513 (north-west Mediterranean Sea). *Journal of Fish Biology* 73, 2402–2420.
514 <https://doi.org/10.1111/j.1095-8649.2008.02093.x>
- 515 Borja, A., Amouroux, D., Anschutz, P., Gómez-Gesteira, M., Uyarra, M.C., Valdés, L.,
516 2019. The bay of biscay, in: *World Seas: An Environmental Evaluation*. Elsevier,
517 pp. 113–152. <https://doi.org/10.1016/B978-0-12-805068-2.00006-1>
- 518 Brind'Amour, A., 2008. NURSE 2008 cruise, Gwen Drez R/V.
519 <https://doi.org/10.17600/8050080>
- 520 Brosset, P., Ménard, F., Fromentin, J.-M., Bonhommeau, S., Ulses, C., Bourdeix, J.-
521 H., Bigot, J.-L., Beveren, E.V., Roos, D., Sarau, C., 2015. Influence of
522 environmental variability and age on the body condition of small pelagic fish in
523 the Gulf of Lions. *Marine Ecology Progress Series* 529, 219–231.
524 <https://doi.org/10.3354/meps11275>
- 525 Bryant, A.D., Heath, M.R., Broekhuizen, N., Ollason, J.G., Gurney, W.S.C.,
526 Greenstreet, S.P.R., 1995. Modelling the predation, growth and population
527 dynamics of fish within a spatially-resolved shelf-sea ecosystem model.
528 *Netherlands Journal of Sea Research* 33, 407–421.
529 [https://doi.org/10.1016/0077-7579\(95\)90055-1](https://doi.org/10.1016/0077-7579(95)90055-1)
- 530 Butenschön, M., Clark, J., Aldridge, J.N., Allen, J.I., Artioli, Y., Blackford, J.,
531 Bruggeman, J., Cazenave, P., Ciavatta, S., Kay, S., Lessin, G., van Leeuwen,
532 S., van der Molen, J., de Mora, L., Polimene, L., Sailley, S., Stephens, N.,
533 Torres, R., 2016. ERSEM 15.06: a generic model for marine biogeochemistry
534 and the ecosystem dynamics of the lower trophic levels. *Geosci. Model Dev.* 9,
535 1293–1339. <https://doi.org/10.5194/gmd-9-1293-2016>
- 536 Castro, N., Costa, J.L., Domingos, I., Angélico, M.M., 2013. Trophic ecology of a
537 coastal fish assemblage in Portuguese waters. *Journal of the Marine Biological*
538 *Association of the United Kingdom* 93, 1151–1161.
539 <https://doi.org/10.1017/S0025315412001853>
- 540 Cavraro, F., Bettoso, N., Zucchetta, M., D'Aietti, A., Faresi, L., Franzoi, P., 2019. Body
541 condition in fish as a tool to detect the effects of anthropogenic pressures in
542 transitional waters. *Aquat Ecol* 53, 21–35. [https://doi.org/10.1007/s10452-018-](https://doi.org/10.1007/s10452-018-09670-4)
543 [09670-4](https://doi.org/10.1007/s10452-018-09670-4)
- 544 Chassé, C., Glémarec, M., 1976. Atlas du littoral français : Atlas des fonds meubles du
545 plateau continental Du Golfe de Gascogne. *Cartes biosédimentaires* 28.

- 546 Chen, D., Wang, Y., Melville, B., Huang, H., Zhang, W., 2018. Unified Formula for
547 Critical Shear Stress for Erosion of Sand, Mud, and Sand–Mud Mixtures.
548 Journal of Hydraulic Engineering 144. [https://doi.org/10.1061/\(ASCE\)HY.1943-7900.0001489](https://doi.org/10.1061/(ASCE)HY.1943-7900.0001489)
549
- 550 Chen, Y.-Y., Edgar, G.J., Fox, R.J., 2021. The Nature and Ecological Significance of
551 Epifaunal Communities within Marine Ecosystems, in: Oceanography and
552 Marine Biology. CRC Press, Boca Raton, pp. 585–719.
553 <https://doi.org/10.1201/9781003138846-9>
- 554 Chouvelon, T., Spitz, J., Caurant, F., Mèndez-Fernandez, P., Chappuis, A., Laugier,
555 F., Le Goff, E., Bustamante, P., 2012. Revisiting the use of $\delta^{15}\text{N}$ in meso-scale
556 studies of marine food webs by considering spatio-temporal variations in stable
557 isotopic signatures – The case of an open ecosystem: The Bay of Biscay (North-
558 East Atlantic). Progress in Oceanography 101, 92–105.
559 <https://doi.org/10.1016/j.pocean.2012.01.004>
- 560 Cormon, X., Ernande, B., Kempf, A., Vermard, Y., Marchal, P., 2016. North Sea saithe
561 *Pollachius virens* growth in relation to food availability, density dependence and
562 temperature. Marine Ecology Progress Series 542, 141–151.
563 <https://doi.org/10.3354/meps11559>
- 564 Corrales, X., Preciado, I., Gascuel, D., Lopez de Gamiz-Zearra, A., Hervann, P.-Y.,
565 Mugerza, E., Louzao, M., Velasco, F., Doray, M., López-López, L., Carrera, P.,
566 Cotano, U., Andonegi, E., 2022. Structure and functioning of the Bay of Biscay
567 ecosystem: A trophic modelling approach. Estuarine, Coastal and Shelf Science
568 264, 107658. <https://doi.org/10.1016/j.ecss.2021.107658>
- 569 Cresson, P., Chouvelon, T., Bustamante, P., Bănar, D., Baudrier, J., Le Loc'h, F.,
570 Mauffret, A., Mialet, B., Spitz, J., Wessel, N., Briand, M.J., Denamiel, M., Doray,
571 M., Guillou, G., Jadaud, A., Lazard, C., Prieur, S., Rouquette, M., Saraux, C.,
572 Serre, S., Timmerman, C.-A., Verin, Y., Harmelin-Vivien, M., 2020. Primary
573 production and depth drive different trophic structure and functioning of fish
574 assemblages in French marine ecosystems. Progress in Oceanography 186,
575 102343. <https://doi.org/10.1016/j.pocean.2020.102343>
- 576 Day, L., Kopp, D., Robert, M., Le Bris, H., 2019. Trophic ecology of large gadiforms in
577 the food web of a continental shelf ecosystem. Progress in Oceanography 175,
578 105–114. <https://doi.org/10.1016/j.pocean.2019.03.007>
- 579 Day, L., Le Bris, H., Saulnier, E., Pinsivy, L., Brind'Amour, A., 2020. Benthic prey
580 production index estimated from trawl survey supports the food limitation
581 hypothesis in coastal fish nurseries. Estuarine, Coastal and Shelf Science 235,
582 106594. <https://doi.org/10.1016/j.ecss.2020.106594>
- 583 Degraer, S., Verfaillie, E., Willems, W., Adriaens, E., Vincx, M., Van Lancker, V., 2008.
584 Habitat suitability modelling as a mapping tool for macrobenthic communities:
585 An example from the Belgian part of the North Sea. Continental Shelf Research
586 28, 369–379. <https://doi.org/10.1016/j.csr.2007.09.001>
- 587 Déniel, C., 1981. Les Poissons plats (Téléostéens, Pleuronectiformes) en baie de
588 Douarnenez: reproduction, croissance et migration des Bothidae,
589 Scophthalmidae, Pleuronectidae et Soleidae. Université de Bretagne
590 occidentale - Brest.
- 591 Deubel, H., Engel, M., Fetzer, I., Gagayev, S., Hirche, H.-J., Klages, M., Larionov, V.,
592 Lubin, P., Lubina, O., Nöthig, E.-M., Okolodkov, Y., Rachor, E., 2003. The Kara
593 Sea ecosystem: phytoplankton, zooplankton and benthos communities
594 influenced by river run-off. Proceedings in Marine Sciences no. 6, Elsevier, pp.
595 237–266.

596 Dubois, S., 2010a. PLOOPS 1 cruise,Thalia R/V. <https://doi.org/10.17600/10070020>

597 Dubois, S., 2010b. PLOOPS 2 cruise,Thalia R/V. <https://doi.org/10.17600/10070090>

598 Dulvy, N.K., Rogers, S.I., Jennings, S., Stelzenmüller, V., Dye, S.R., Skjoldal, H.R.,
599 2008. Climate change and deepening of the North Sea fish assemblage: a biotic
600 indicator of warming seas. *Journal of Applied Ecology* 45, 1029–1039.
601 <https://doi.org/10.1111/j.1365-2664.2008.01488.x>

602 Dutertre, M., Hamon, D., Chevalier, C., Ehrhold, A., 2013. The use of the relationships
603 between environmental factors and benthic macrofaunal distribution in the
604 establishment of a baseline for coastal management. *ICES Journal of Marine
605 Science* 70, 294–308. <https://doi.org/10.1093/icesjms/fss170>

606 Ehrnsten, E., Norkko, A., Timmermann, K., Gustafsson, B.G., 2019. Benthic-pelagic
607 coupling in coastal seas – Modelling macrofaunal biomass and carbon
608 processing in response to organic matter supply. *Journal of Marine Systems*
609 196, 36–47. <https://doi.org/10.1016/j.jmarsys.2019.04.003>

610 Engelhard, G.H., Blanchard, J.L., Pinnegar, J.K., van der Kooij, J., Bell, E.D.,
611 Mackinson, S., Righton, D.A., 2013. Body condition of predatory fishes linked to
612 the availability of sandeels. *Mar Biol* 160, 299–308.
613 <https://doi.org/10.1007/s00227-012-2088-1>

614 Escobar-Briones, E.G., Soto, L.A., 1997. Continental shelf benthic biomass in the
615 western Gulf of Mexico. *Continental Shelf Research* 17, 585–604.
616 [https://doi.org/10.1016/S0278-4343\(96\)00047-7](https://doi.org/10.1016/S0278-4343(96)00047-7)

617 Fanelli, E., Principato, E., Monfardini, E., Da Ros, Z., Scarcella, G., Santojanni, A.,
618 Colella, S., 2022. Seasonal Trophic Ecology and Diet Shift in the Common Sole
619 *Solea solea* in the Central Adriatic Sea. *Animals* 12, 3369.
620 <https://doi.org/10.3390/ani12233369>

621 GEBCO Bathymetric Compilation Group, 2023. GEBCO 2023 Grid.
622 <https://doi.org/10.5285/F98B053B-0CBC-6C23-E053-6C86ABC0AF7B>

623 Gibson, R.N., Ezzi, I.A., 1980. The biology of the scaldfish, *Arnoglossus laterna*
624 (Walbaum) on the west coast of Scotland. *Journal of Fish Biology* 17, 565–575.
625 <https://doi.org/10.1111/j.1095-8649.1980.tb02788.x>

626 Glémarec, M., 1969. Les Peuplements benthiques du plateau continental nord-
627 Gascogne. Atelier offset de la Faculté des sciences, Brest, France.

628 Hall, S.J., 2002. The continental shelf benthic ecosystem: current status, agents for
629 change and future prospects. *Envir. Conserv.* 29, 350–374.
630 <https://doi.org/10.1017/S0376892902000243>

631 Hiddink, J.G., Moranta, J., Balestrini, S., Sciberras, M., Cendrier, M., Bowyer, R.,
632 Kaiser, M.J., Sköld, M., Jonsson, P., Bastardie, F., Hinz, H., 2016. Bottom
633 trawling affects fish condition through changes in the ratio of prey availability to
634 density of competitors. *Journal of Applied Ecology* 53, 1500–1510.
635 <https://doi.org/10.1111/1365-2664.12697>

636 Hijmans, R.J., 2023. raster: Geographic Data Analysis and Modeling.

637 Hislop, J.R.G., Robb, A.P., Bell, M.A., Armstrong, D.W., 1991. The diet and food
638 consumption of whiting (*Merlangius merlangus*) in the North Sea. *ICES Journal
639 of Marine Science* 48, 139–156. <https://doi.org/10.1093/icesjms/48.2.139>

640 Holbrook, S.J., Schmitt, R.J., 1989. Resource Overlap, Prey Dynamics, and The
641 Strength of Competition. *Ecology* 70, 1943–1953.
642 <https://doi.org/10.2307/1938124>

643 Idier, D., Romieu, E., Pedreros, R., Oliveros, C., 2010. A simple method to analyse
644 non-cohesive sediment mobility in coastal environment. *Continental Shelf
645 Research* 30, 365–377. <https://doi.org/10.1016/j.csr.2009.12.006>

- 646 Kamimura, Y., Taga, M., Yukami, R., Watanabe, C., Furuichi, S., 2021. Intra- and inter-
647 specific density dependence of body condition, growth, and habitat temperature
648 in chub mackerel (*Scomber japonicus*). *ICES Journal of Marine Science* 78,
649 3254–3264. <https://doi.org/10.1093/icesjms/fsab191>
- 650 Karlson, A., Reutgard, M., Garbaras, A., Gorokhova, E., 2018. Isotopic niche reflects
651 stress-induced variability in physiological status. *Royal Society Open Science*
652 5, 171398. <https://doi.org/10.1098/rsos.171398>
- 653 Kaskela, A.M., Kotilainen, A.T., Alanen, U., Cooper, R., Green, S., Guinan, J., van
654 Heteren, S., Kihlman, S., Van Lancker, V., Stevenson, A., the EMODnet
655 Geology Partners, 2019. Picking Up the Pieces—Harmonising and Collating
656 Seabed Substrate Data for European Maritime Areas. *Geosciences* 9, 84.
657 <https://doi.org/10.3390/geosciences9020084>
- 658 Kay, S., Andersson, H., Eilola, K., Wehde, H., Ramirez-Romero, E., Jordà, G., Catalan,
659 I., 2018. Climate change and European aquatic resources (CERES) deliverable
660 D1.3 projections of physical and biogeochemical parameters and habitat
661 indicators for European seas, including synthesis of sea level rise and
662 storminess., CERES report.
- 663 King, P.A., Fives, J.M., 1990. Littoral and Benthic Investigations on the West Coast of
664 Ireland: XXIII. A Contribution to the Biology of the Thick-Back Sole *Microchirus*
665 *variegatus* (Donovan, 1808) in the Galway Bay Area. *Proceedings of the Royal*
666 *Irish Academy. Section B: Biological, Geological, and Chemical Science* 90B,
667 23–31.
- 668 Kopp, D., Lefebvre, S., Cachera, M., Villanueva, M.C., Ernande, B., 2015.
669 Reorganization of a marine trophic network along an inshore–offshore gradient
670 due to stronger pelagic–benthic coupling in coastal areas. *Progress in*
671 *Oceanography* 130, 157–171. <https://doi.org/10.1016/j.pocean.2014.11.001>
- 672 Laffargue, P., 2013a. FEBBE 1 cruise, Gwen Drez R/V.
673 <https://doi.org/10.17600/13050040>
- 674 Laffargue, P., 2013b. FEBBE 2 cruise, Gwen Drez R/V.
675 <https://doi.org/10.17600/13050050>
- 676 Laffargue, P., Garren, F., Duhamel, E., 2020. EVHOE 2020 cruise.
677 <https://doi.org/10.17600/18000661>
- 678 Lagardère, J.P., 1987. Feeding ecology and daily food consumption of common sole,
679 *Solea vulgaris* Quensel, juveniles on the French Atlantic coast. *Journal of Fish*
680 *Biology* 30, 91–104. <https://doi.org/10.1111/j.1095-8649.1987.tb05735.x>
- 681 Lassalle, G., Lobry, J., Le Loc'h, F., Bustamante, P., Certain, G., Delmas, D., Dupuy,
682 C., Hily, C., Labry, C., Le Pape, O., Marquis, E., Petitgas, P., Pusineri, C.,
683 Ridoux, V., Spitz, J., Niquil, N., 2011. Lower trophic levels and detrital biomass
684 control the Bay of Biscay continental shelf food web: Implications for ecosystem
685 management. *Progress in Oceanography* 91, 561–575.
686 <https://doi.org/10.1016/j.pocean.2011.09.002>
- 687 Laurel, B. j., Brown, J.A., Anderson, R., 2001. Behaviour, growth and survival of redfish
688 larvae in relation to prey availability. *Journal of Fish Biology* 59, 884–901.
689 <https://doi.org/10.1111/j.1095-8649.2001.tb00159.x>
- 690 Le Bec, C., 1983. Cycle sexuel et fécondité de la sole *Solea vulgaris* (Quensel, 1806)
691 du Golfe de Gascogne. *Revue des Travaux de l'Institut des Pêches Maritimes*
692 47, 179–189.
- 693 Le Bris, H., 2010. ISOBAIE 2 cruise, Gwen Drez R/V.
694 <https://doi.org/10.17600/10050050>
- 695 Le Bris, H., 2008. RETROB cruise, Gwen Drez R/V. <https://doi.org/10.17600/8050020>

- 696 Le Bris, H., Glémarec, M., 1995. Macrozoobenthic communities of an oxygen under-
697 saturated coastal ecosystem: The Bay of Vilaine (southern Brittany).
698 *Oceanologica Acta* 18, 573–581.
- 699 Le Cren, E.D., 1951. The Length-Weight Relationship and Seasonal Cycle in Gonad
700 Weight and Condition in the Perch (*Perca fluviatilis*). *The Journal of Animal*
701 *Ecology* 20, 201. <https://doi.org/10.2307/1540>
- 702 Le Loc'h, F., Grall, J., 2019. APPEAL ATL 19-2 cruise, Côtes De La Manche R/V.
703 <https://doi.org/10.17600/18001062>
- 704 Le Loc'h, F., Grall, J., 2018a. APPEAL ATL 18-1 cruise, Côtes De La Manche R/V.
705 <https://doi.org/10.17600/18001061>
- 706 Le Loc'h, F., Grall, J., 2018b. APPEAL ATL 18-2 cruise, Côtes De La Manche R/V.
707 <https://doi.org/10.17600/18000466>
- 708 Le Loc'h, F., Hily, C., 2005. Stable carbon and nitrogen isotope analysis of *Nephrops*
709 *norvegicus* / *Merluccius merluccius* fishing grounds in the Bay of Biscay
710 (Northeast Atlantic). *Can. J. Fish. Aquat. Sci.* 62, 123–132.
711 <https://doi.org/10.1139/f04-242>
- 712 Le Loc'h, F., Hily, C., Grall, J., 2008. Benthic community and food web structure on the
713 continental shelf of the Bay of Biscay (North Eastern Atlantic) revealed by stable
714 isotopes analysis. *Journal of Marine Systems* 72, 17–34.
715 <https://doi.org/10.1016/j.jmarsys.2007.05.011>
- 716 Liao, H., Pierce, C.L., Wahl, D.H., Rasmussen, J.B., Leggett, W.C., 1995. Relative
717 Weight (W) as a Field Assessment Tool: Relationships with Growth, Prey
718 Biomass, and Environmental Conditions. *Transactions of the American*
719 *Fisheries Society* 124, 387–400. [https://doi.org/10.1577/1548-8659\(1995\)124<0387:RWWRAA>2.3.CO;2](https://doi.org/10.1577/1548-8659(1995)124<0387:RWWRAA>2.3.CO;2)
- 721 Lopez De Gamiz-Zearra, A., Hansen, C., Corrales, X., Quincoces, I., Preciado, I.,
722 Andonegi, E., 2023. Parameterization and tuning of the Bay of Biscay Atlantis
723 model v1. <https://doi.org/10.5194/egusphere-2023-1368>
- 724 McArthur, M.A., Brooke, B.P., Przeslawski, R., Ryan, D.A., Lucieer, V.L., Nichol, S.,
725 McCallum, A.W., Mellin, C., Cresswell, I.D., Radke, L.C., 2010. On the use of
726 abiotic surrogates to describe marine benthic biodiversity. *Estuarine, Coastal*
727 *and Shelf Science* 88, 21–32. <https://doi.org/10.1016/j.ecss.2010.03.003>
- 728 N'Da, K., Déniel, C., 1993. Sexual cycle and seasonal changes in the ovary of the red
729 mullet, *Mullus surmuletus*, from the southern coast of Brittany. *Journal of Fish*
730 *Biology* 43, 229–244. <https://doi.org/10.1111/j.1095-8649.1993.tb00425.x>
- 731 Pace, M.C., Bailey, D.M., Donnan, D.W., Narayanaswamy, B.E., Smith, H.J., Speirs,
732 D.C., Turrell, W.R., Heath, M.R., 2021. Modelling seabed sediment physical
733 properties and organic matter content in the Firth of Clyde.
734 <https://doi.org/10.5194/essd-2021-23>
- 735 Pavičić, M., Šiljić, J., Jurica, D.B., Matic-Skoko, S., 2018. Feeding habits of the striped
736 red mullet, *Mullus surmuletus* in the eastern Adriatic Sea. *Acta Adriatica* 59,
737 123–136. <https://doi.org/10.32582/aa.59.1.10>
- 738 Pearson, T., Rosenberg, R., 1978. Macrobenthic succession in relation to organic
739 enrichment and pollution of the marine environment. *Oceanography and Marine*
740 *Biology* 16, 229–311.
- 741 Pebesma, E., 2018. Simple Features for R: Standardized Support for Spatial Vector
742 Data. *The R Journal* 10, 439. <https://doi.org/10.32614/RJ-2018-009>
- 743 Pelage, L., Lucena-Frédou, F., Eduardo, L.N., Le Loc'h, F., Bertrand, A., Lira, A.S.,
744 Frédou, T., 2022. Competing with each other: Fish isotopic niche in two

745 resource availability contexts. *Front. Mar. Sci.* 9.
746 <https://doi.org/10.3389/fmars.2022.975091>

747 Peña, M., González-Quirós, R., Munuera-Fernández, I., González, F., Romero-
748 Romero, S., Nogueira, E., 2019. Vertical distribution and aggregation patterns
749 of krill (Crustacea: Euphausiacea) in the Bay of Biscay: interannual and
750 seasonal variability. *Can. J. Zool.* 97, 619–630. <https://doi.org/10.1139/cjz-2018-0119>

751
752 Pierrejean, M., Laffargue, P., Desroy, N., 2022. Test de déploiement des suivis du
753 compartiment de la macrofaune benthique sur les fonds meubles du plateau via
754 les campagnes halieutiques de l'Ifremer, au titre de la DCSMM. Ifremer.
755 <https://doi.org/10.13155/92737>

756 Porath, M.T., Peters, E.J., 1997. Use of Walleye Relative Weights (W) to Assess Prey
757 Availability. *North American Journal of Fisheries Management* 17, 628–637.
758 [https://doi.org/10.1577/1548-8675\(1997\)017<0628:UOWRWW>2.3.CO;2](https://doi.org/10.1577/1548-8675(1997)017<0628:UOWRWW>2.3.CO;2)

759 Qin, X.-B., Sun, H.-W., Wu, J.-Z., Wang, R.-N., Sun, T.-H., 2010. Bioturbation of
760 macrobenthos on estuarine sediment. *Ying Yong Sheng Tai Xue Bao* 21, 458–
761 463.

762 R core team, 2023. R: A language and environment for statistical computing. R
763 Foundation for Statistical Computing, Vienna, Austria. [WWW Document]. URL
764 <https://www.r-project.org/> (accessed 12.20.22).

765 Rault, J., Le Bris, H., Robert, M., Pawlowski, L., Denamiel, M., Kopp, D., 2017. Diets
766 and trophic niches of the main commercial fish species from the Celtic Sea.
767 *Journal of Fish Biology* 91, 1449–1474. <https://doi.org/10.1111/jfb.13470>

768 Reiss, H., Birchenough, S., Borja, A., Buhl-Mortensen, L., Craeymeersch, J.,
769 Dannheim, J., Darr, A., Galparsoro, I., Gogina, M., Neumann, H., Populus, J.,
770 Rengstorf, A.M., Valle, M., van Hoey, G., Zettler, M.L., Degraer, S., 2015.
771 Benthos distribution modelling and its relevance for marine ecosystem
772 management. *ICES Journal of Marine Science* 72, 297–315.
773 <https://doi.org/10.1093/icesjms/fsu107>

774 Reiss, H., Degraer, S., Duineveld, G.C.A., Kröncke, I., Aldridge, J., Craeymeersch,
775 J.A., Eggleton, J.D., Hillewaert, H., Lavaleye, M.S.S., Moll, A., Pohlmann, T.,
776 Rachor, E., Robertson, M., Vanden Berghe, E., van Hoey, G., Rees, H.L., 2010.
777 Spatial patterns of infauna, epifauna, and demersal fish communities in the
778 North Sea. *ICES Journal of Marine Science* 67, 278–293.
779 <https://doi.org/10.1093/icesjms/fsp253>

780 Rigolet, C., Dubois, S.F., Thiébaud, E., 2014. Benthic control freaks: Effects of the
781 tubicolous amphipod *Haploops nirae* on the specific diversity and functional
782 structure of benthic communities. *Journal of Sea Research* 85, 413–427.
783 <https://doi.org/10.1016/j.seares.2013.07.013>

784 Rijnsdorp, A.D., 1990. The mechanism of energy allocation over reproduction and
785 somatic growth in female North Sea plaice, *Pleuronectes platessa* L.
786 *Netherlands Journal of Sea Research* 25, 279–289.
787 [https://doi.org/10.1016/0077-7579\(90\)90027-E](https://doi.org/10.1016/0077-7579(90)90027-E)

788 Robert, A., 2017. Effets combinés des facteurs naturels et anthropiques sur la diversité
789 fonctionnelle des vasières à langoustines (*Nephrops norvegicus*) du golfe de
790 Gascogne (phdthesis). Agrocampus Ouest.

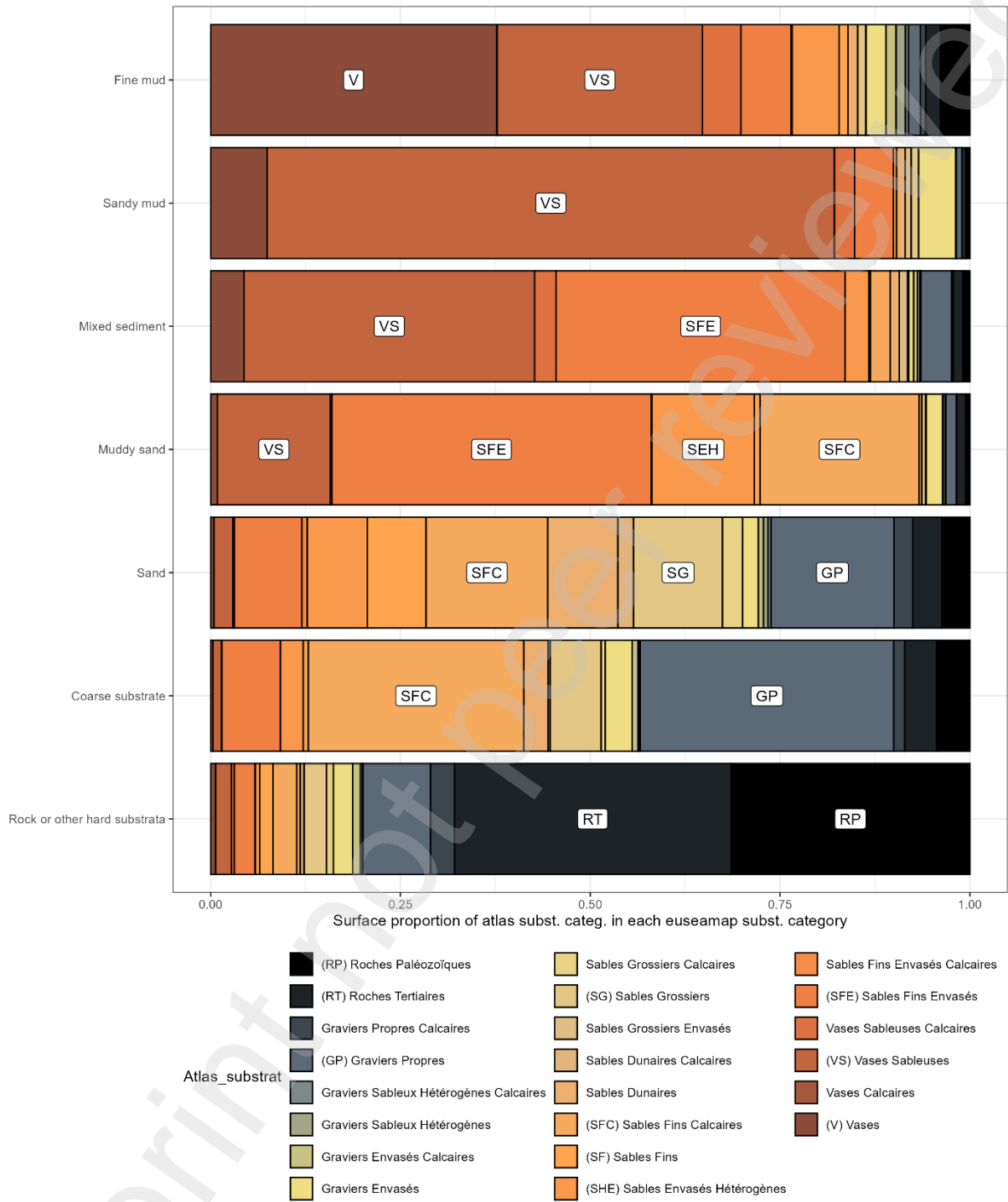
791 Rodríguez-Cabello, C., Sánchez, F., Olaso, I., 2007. Distribution patterns and sexual
792 segregations of *Scylliorhinus canicula* (L.) in the Cantabrian Sea. *Journal of Fish
793 Biology* 70, 1568–1586. <https://doi.org/10.1111/j.1095-8649.2007.01444.x>

- 794 Sánchez-Hernández, J., Hayden, B., Harrod, C., Kahilainen, K.K., 2021. Population
795 niche breadth and individual trophic specialisation of fish along a climate-
796 productivity gradient. *Rev Fish Biol Fisheries* 31, 1025–1043.
797 <https://doi.org/10.1007/s11160-021-09687-3>
- 798 Šantić, M., Rađa, B., Pallaoro, A., 2012. Feeding habits of small-spotted catshark
799 (*Scyliorhinus canicula* Linnaeus, 1758) from the eastern central Adriatic Sea.
800 *Marine Biology Research* 8, 1003–1011.
801 <https://doi.org/10.1080/17451000.2012.702912>
- 802 Schloesser, R.W., Fabrizio, M.C., 2019. Nursery Habitat Quality Assessed by the
803 Condition of Juvenile Fishes: Not All Estuarine Areas Are Equal. *Estuaries and*
804 *Coasts* 42, 548–566. <https://doi.org/10.1007/s12237-018-0468-6>
- 805 Schückel, S., Sell, A., Kröncke, I., Reiss, H., 2011. Diet composition and resource
806 partitioning in two small flatfish species in the German Bight. *Journal of Sea*
807 *Research* 66, 195–204. <https://doi.org/10.1016/j.seares.2011.06.003>
- 808 Serrano, A., Velasco, F., Olaso, I., Sánchez, F., 2003. Macrobenthic crustaceans in
809 the diet of demersal fish in the Bay of Biscay in relation to abundance in the
810 environment. *Sarsia* 88, 36–48. <https://doi.org/10.1080/00364820308469>
- 811 Simpson, J.H., Sharples, J. (Eds.), 2012. The shelf edge system, in: *Introduction to the*
812 *Physical and Biological Oceanography of Shelf Seas*. Cambridge University
813 Press, Cambridge, pp. 304–351.
814 <https://doi.org/10.1017/CBO9781139034098.013>
- 815 Sorbe, J.C., 1981. Rôle du benthos dans le régime alimentaire des poissons démersaux
816 du secteur Sud Gascogne. *Kieler Meeresforschungen - Sonderheft* 5, 479–489.
- 817 Souissi, S., Ibanez, F., Hamadou, R.B., Boucher, J., Cathelineau, A.C., Blanchard, F.,
818 Poulard, J.-C., 2001. A new multivariate mapping method for studying species
819 assemblages and their habitats: Example using bottom trawl surveys in the Bay
820 of Biscay (France). *Sarsia* 86, 527–542.
821 <https://doi.org/10.1080/00364827.2001.10420491>
- 822 Timmermann, K., Norkko, J., Janas, U., Norkko, A., Gustafsson, B.G., Bonsdorff, E.,
823 2012. Modelling macrofaunal biomass in relation to hypoxia and nutrient
824 loading. *Journal of Marine Systems* 105–108, 60–69.
825 <https://doi.org/10.1016/j.jmarsys.2012.06.001>
- 826 Vandromme, P., Nogueira, E., Huret, M., Lopez-Urrutia, & Aacute;, González-
827 Nuevo González, G., Sourisseau, M., Petitgas, P., 2014. Springtime
828 zooplankton size structure over the continental shelf of the Bay of Biscay. *Ocean*
829 *Sci.* 10, 821–835. <https://doi.org/10.5194/os-10-821-2014>
- 830 Wei, C.-L., Rowe, G.T., Escobar-Briones, E., Boetius, A., Soltwedel, T., Caley, M.J.,
831 Soliman, Y., Huettmann, F., Qu, F., Yu, Z., Pitcher, C.R., Haedrich, R.L.,
832 Wicksten, M.K., Rex, M.A., Baguley, J.G., Sharma, J., Danovaro, R.,
833 MacDonald, I.R., Nunnally, C.C., Deming, J.W., Montagna, P., Lévesque, M.,
834 Weslawski, J.M., Wlodarska-Kowalczyk, M., Ingole, B.S., Bett, B.J., Billett,
835 D.S.M., Yool, A., Bluhm, B.A., Iken, K., Narayanaswamy, B.E., 2010. Global
836 Patterns and Predictions of Seafloor Biomass Using Random Forests. *PLoS*
837 *ONE* 5, e15323. <https://doi.org/10.1371/journal.pone.0015323>
- 838 Zhang, Y., Cheng, L., Li, K., Zhang, L., Cai, Y., Wang, X., Heino, J., 2019. Nutrient
839 enrichment homogenizes taxonomic and functional diversity of benthic
840 macroinvertebrate assemblages in shallow lakes. *Limnology and*
841 *Oceanography* 64, 1047–1058. <https://doi.org/10.1002/lno.11096>

842 Zuschin, M., Stachowitsch, M., 2009. Epifauna-dominated benthic shelf assemblages:
843 lessons from the modern adriatic sea. PALAIOS 24, 211–221.
844 <https://doi.org/10.2110/palo.2008.p08-062r>

845 Zuur, A.F., Ieno, E.N., Walker, N., Saveliev, A.A., Smith, G.M., 2009. Mixed effects
846 models and extensions in ecology with R, Statistics for Biology and Health.
847 Springer New York, New York, NY. <https://doi.org/10.1007/978-0-387-87458-6>
848

849



851

852 *Figure SM1: Relative proportion of the area of each Atlas map substrate polygon contained in each*
 853 *Euseamap substrate polygon.*

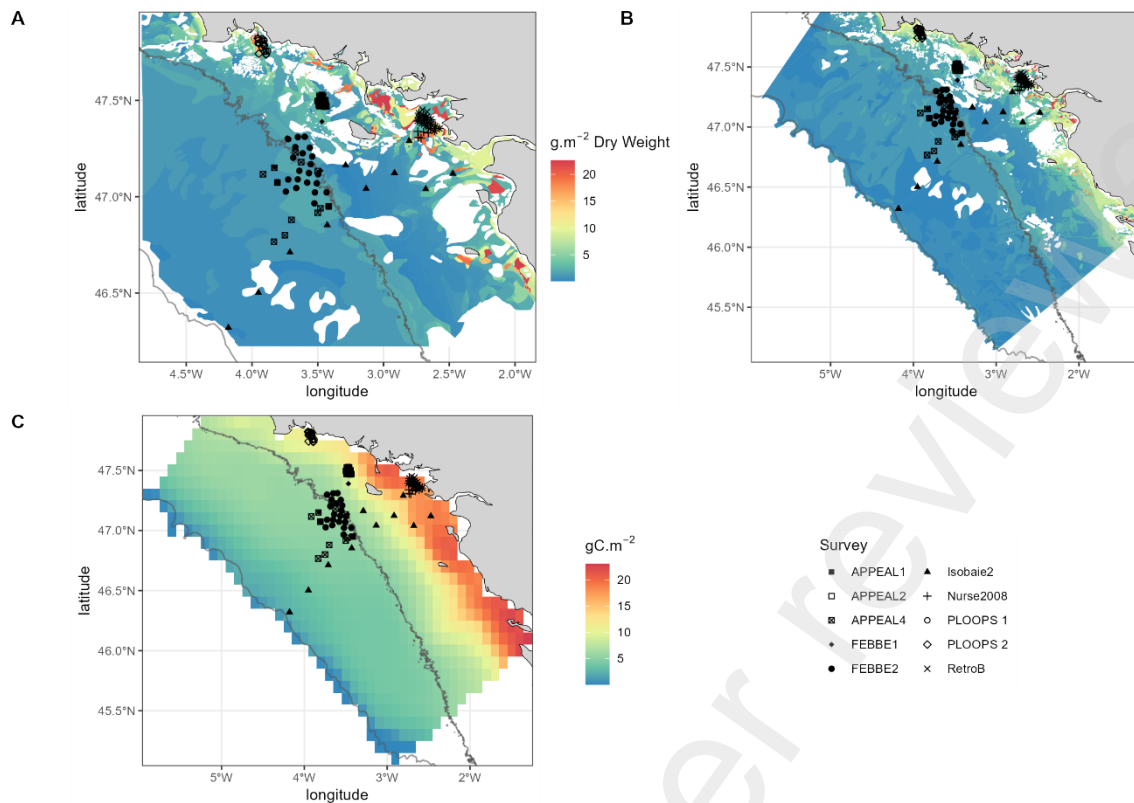
854

855 Table SM2: Different substrate categories of different substrate maps and the correspondence between
 856 them and the graph model.

Graph	model	Atlas biosedimentary substrate categories	Euseamap	substrate
substrate categories			categories	
		Roches Paléozoïques ; Roches Tertiaires		Rock or other hard substrata; Seabed; Worm reefs
GP-GV		Graviers Envasés ; Graviers Envasés Calcaires ; Graviers Propres ; Graviers Propres Calcaires		Coarse substrate
GH		Graviers Sableux Hétérogènes ; Graviers Sableux Hétérogènes Calcaires		
SG		Sables Grossiers ; Sables Grossiers Calcaires		Coarse substrate
SF		Sables Dunaires ; Sables Dunaires Calcaires ; Sables Fins ; Sables Fins Calcaires		Sand
SHV		Sables Envasés Hétérogènes ; Sables Grossiers Envasés		
FV		Sables Fins Envasés ; Sables Fins Envasés Calcaires		Muddy sand
VS		Vases Sableuses ; Vases Sableuses Calcaires		Mixed sediment Sandy mud
VV		Vases ; Vases Calcaires		Fine mud

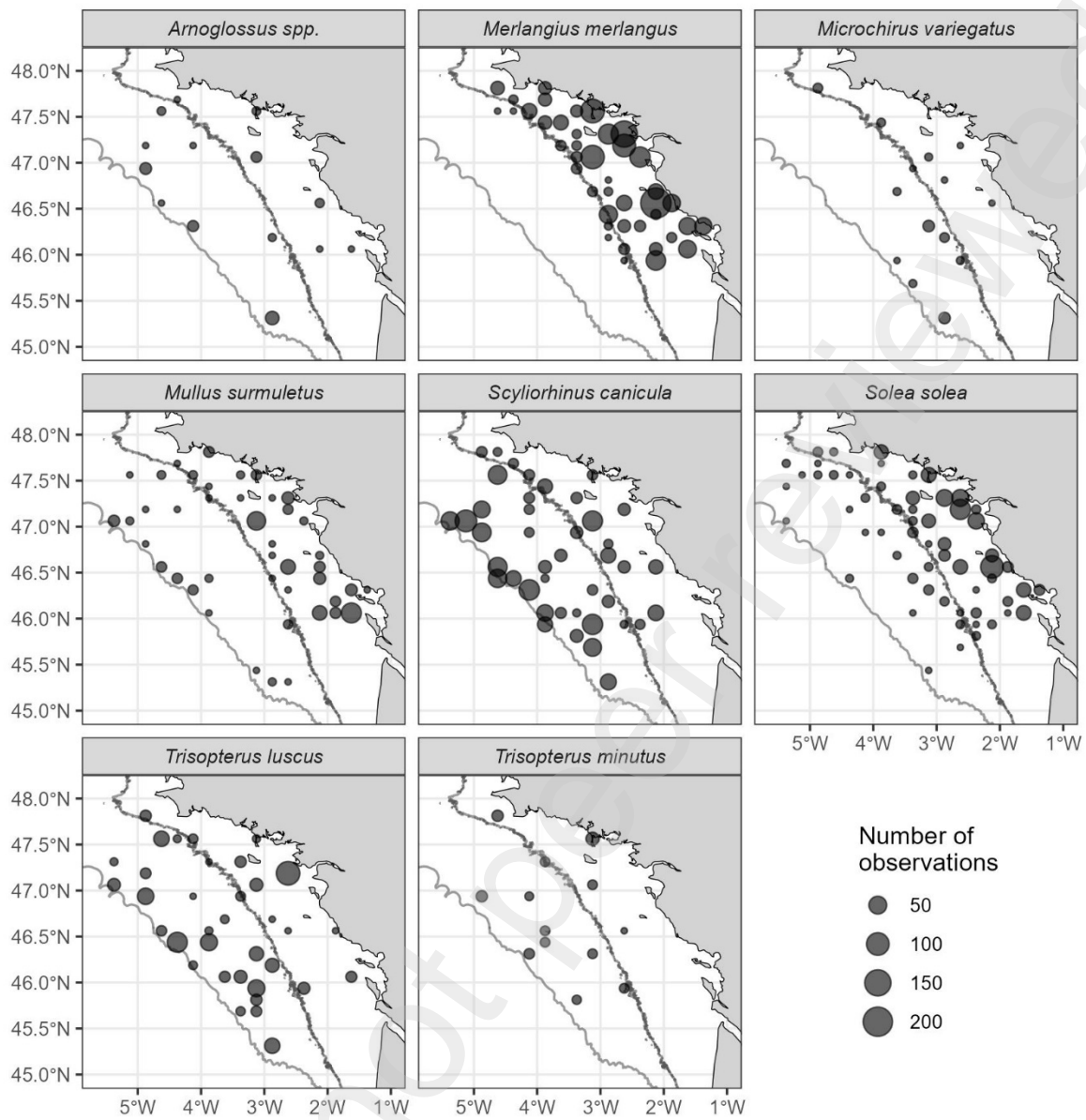
857

858



859

860 *Figure SM3: The location of sampling stations from various surveys along the continental shelf of the*
 861 *Bay of Biscay. Panel A depicts values of the macrobenthic biomass index obtained from the graph model*
 862 *based on 'Atlas' substrate maps, B shows values from the graph model based on a recent substrate*
 863 *map, and C is the average biomass of suspension and deposit feeders estimated by the POLCOMS-*
 864 *ERSEM model between 2006–2015. Gray lines represent the 100- and 200-meter isobaths.*



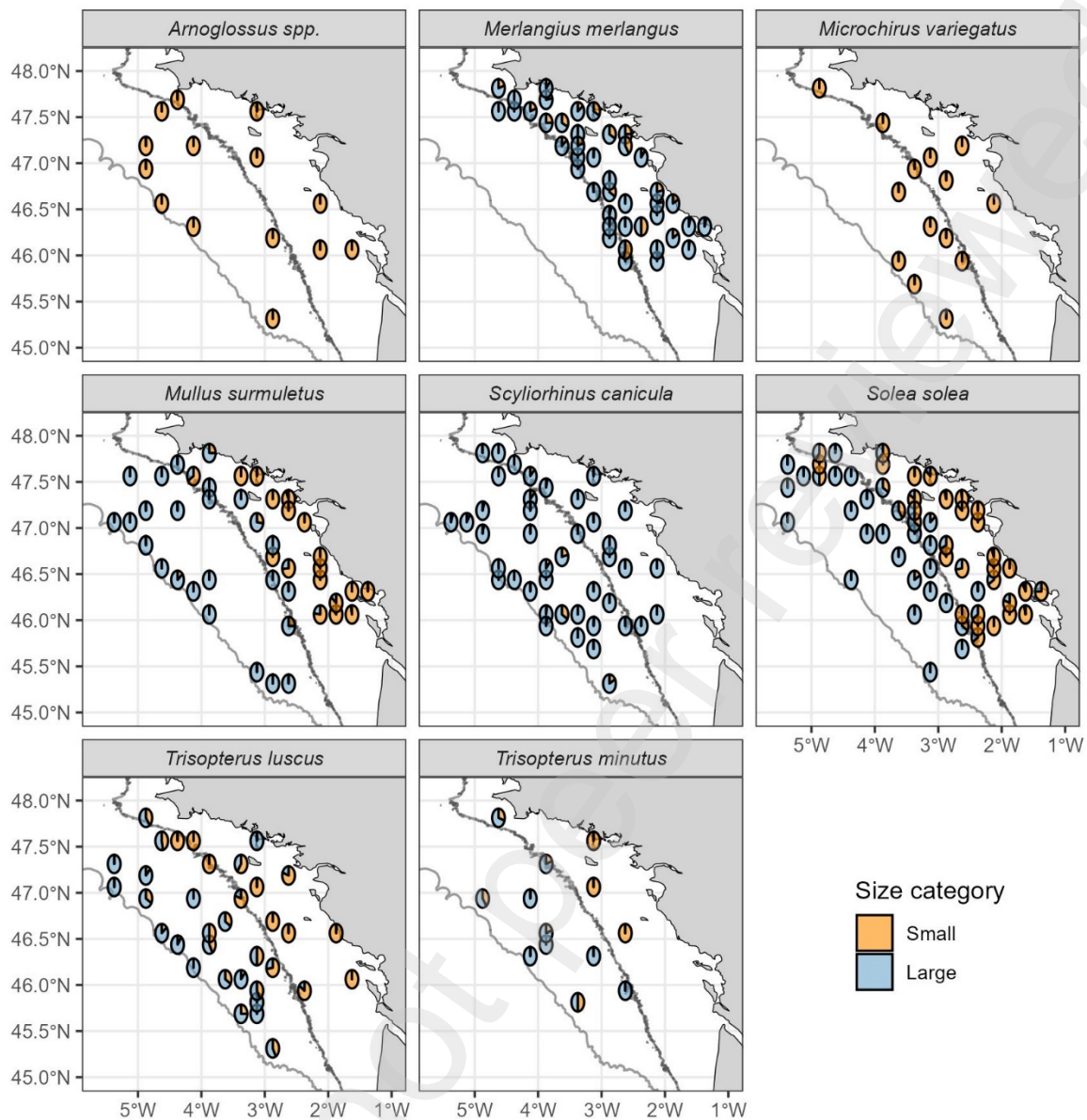
865

866

867

868

Figure SM4: Spatial distribution of available data on benthic-demersal fish condition. Gray lines represent the 100- and 200-meter isobaths.



869

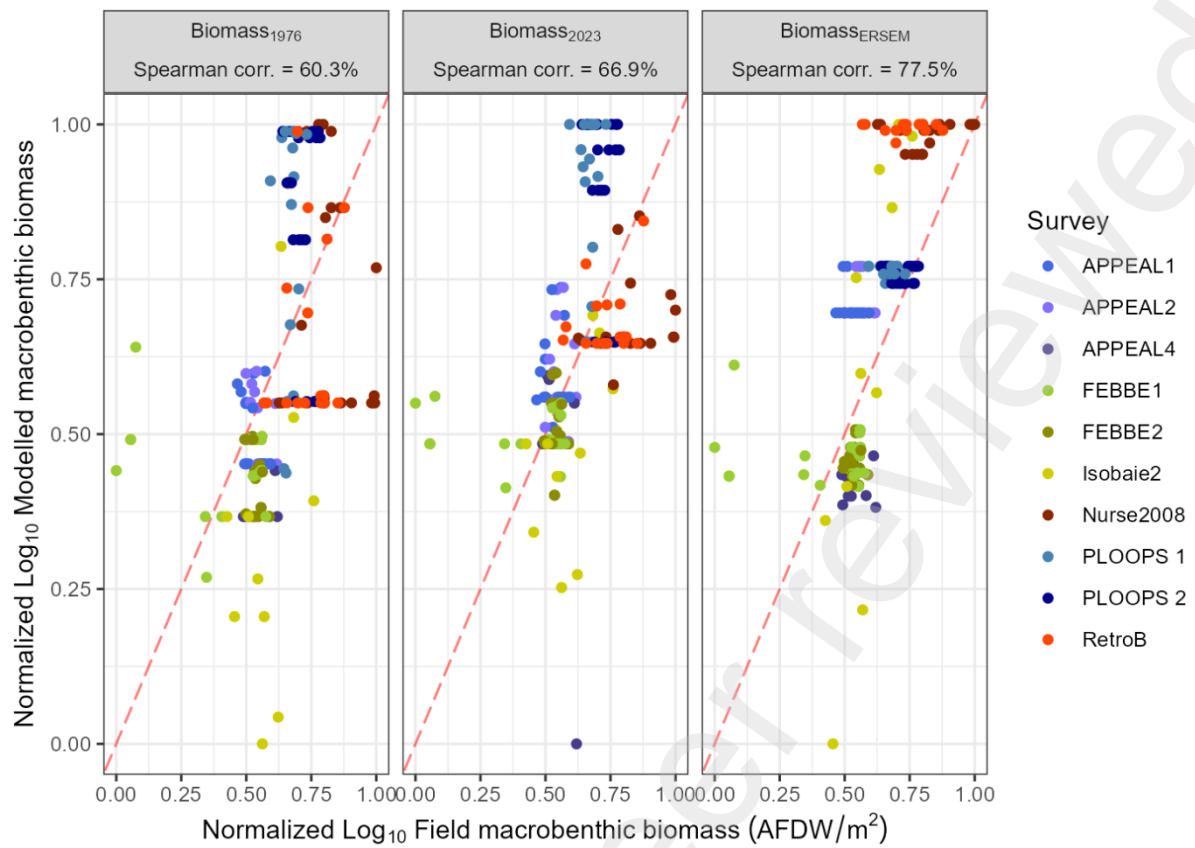
870 *Figure SM5: Relative proportion of 'Small' and 'Large' size-class categories in the available data on*
 871 *bentho-demersal fish condition. Gray lines represent the 100- and 200-meter isobaths.*

872

873 Table SM6: Number of samples included in the analysis, based on the biomass model used—"graph
 874 model" (Biomass₁₉₇₆, Biomass₂₀₂₃) or ERSEM model (Biomass_{ERSEM})—and the fish size categories,
 875 small (S) or large (L).

Species	Number of individuals
<i>Arnoglossus spp.</i>	Biomass ₁₉₇₆ : 45
	Biomass ₂₀₂₃ : 67
	Biomass _{ERSEM} : 67
<i>Merlangius merlangus</i>	Biomass ₁₉₇₆ : 253 (S) & 975 (L)
	Biomass ₂₀₂₃ : 268 (S) & 1192 (L)
	Biomass _{ERSEM} : 268 (S) & 1192 (L)
<i>Microchirus variegatus</i>	Biomass ₁₉₇₆ : 32
	Biomass ₂₀₂₃ : 48
	Biomass _{ERSEM} : 48
<i>Mullus surmuletus</i>	Biomass ₁₉₇₆ : 95 (S) & 91 (L)
	Biomass ₂₀₂₃ : 211 (S) & 123 (L)
	Biomass _{ERSEM} : 211 (S) & 123 (L)
<i>Scyliorhinus canicula</i>	Biomass ₁₉₇₆ : 12 (S) & 683 (L)
	Biomass ₂₀₂₃ : 35 (S) & 1094 (L)
	Biomass _{ERSEM} : 35 (S) & 1098 (L)
<i>Solea solea</i>	Biomass ₁₉₇₆ : 418 (S) & 121 (L)
	Biomass ₂₀₂₃ : 490 (S) & 140 (L)
	Biomass _{ERSEM} : 490 (S) & 140 (L)
<i>Trisopterus luscus</i>	Biomass ₁₉₇₆ : 217 (S) & 204 (L)
	Biomass ₂₀₂₃ : 274 (S) & 309 (L)
	Biomass _{ERSEM} : 274 (S) & 310 (L)

876



877

878 Figure SM7 Biplot of modeled macrobenthic biomass compared to observed macrobenthic biomass.

879 Stations are colored according to their respective survey.

880